Insect Systematics and Diversity, 6(5), 7; 2022, 1–30
https://doi.org/10.1093/isd/ixac021
Research

ENTOMOLOGICAL SOCIETY OF AMERICA
SHARING INSECT SCIENCE GLOBALLY

OXFORD

Evolution

Morphology-based Phylogenetic Analysis of Membracoidea (Hemiptera: Cicadomorpha) With Placement of Fossil Taxa and Description of a New Subfamily

Christopher H. Dietrich,[1,2,6] Dmitry A. Dmitriev,[2] Daniela M. Takiya,[3] M. Jared Thomas,[2] Michael D. Webb,[4] James N. Zahniser,[5] and Yalin Zhang[1,6]

[1]Entomological Museum, College of Plant Protection, Northwest A&F University, Yangling, Shaanxi, China,[2]Illinois Natural History Survey, Prairie Research Institute, University of Illinois, 1816 South Oak Street, Champaign, IL 61820, USA,[3]Departamento de Zoologia, Instituto de Biologia, Universidade Federal do Rio de Janeiro, Rio de Janeiro, RJ, Brazil,[4]The Natural History Museum, Cromwell Road, London SW7 5BD, UK,[5]United States Department of Agriculture, APHIS-PPQ-NIS, MRC-168, National Museum of Natural History, Smithsonian Institution, P.O. Box 37012, Washington, DC 20013-7012, USA, and [6]Corresponding authors, e-mail: chdietri@illinois.edu, yalinzh@nwafu.edu.cn

Subject Editor: Kazunori Yoshizawa

Received 26 April 2022; Editorial decision 29 June 2022

Abstract

Recently discovered amber-preserved fossil Cicadellidae exhibit combinations of morphological traits not observed in the modern fauna and have the potential to shed new light on the evolution of this highly diverse family. To place the fossils explicitly within a phylogenetic context, representatives of five extinct genera from Cretaceous Myanmar amber, and one from Eocene Baltic amber were incorporated into a matrix comprising 229 discrete morphological characters and representatives of all modern subfamilies. Phylogenetic analyses yielded well resolved and largely congruent estimates that support the monophyly of most previously recognized cicadellid subfamilies and indicate that the treehoppers are derived from a lineage of Cicadellidae. Instability in the morphology-based phylogenies is mainly confined to deep internal splits that received low branch support in one or more analyses and also were not consistently resolved by recent phylogenomic analyses. Placement of fossil taxa is mostly stable across analyses. Three new Cretaceous leafhopper genera, *Burmotettix* gen. nov., *Kachinella* gen nov., and *Viraktamathus* gen. nov., consistently form a monophyletic group distinct from extant leafhopper subfamilies and are placed in Burmotettiginae subfam. nov. Extinct Cretaceous fossils previously placed in Ledrinae and Signoretiinae are recovered as sister to modern representatives of these groups. *Eomegophthalmus* Dietrich and Gonçalves from Baltic amber consistently groups with a lineage comprising treehoppers, Megophthalminae, Ulopinae, and Eurymelinae but its position is unstable. Overall, the morphology-based phylogenetic estimates agree with recent phylogenies based on molecular data alone suggesting that morphological traits recently used to diagnose subfamilies are generally informative of phylogenetic relationships within this group.

Version of Record, frst published online October 31, 2022 with fxed content and layout in compliance with Art. 8.1.3.2 ICZN

Graphical Abstract

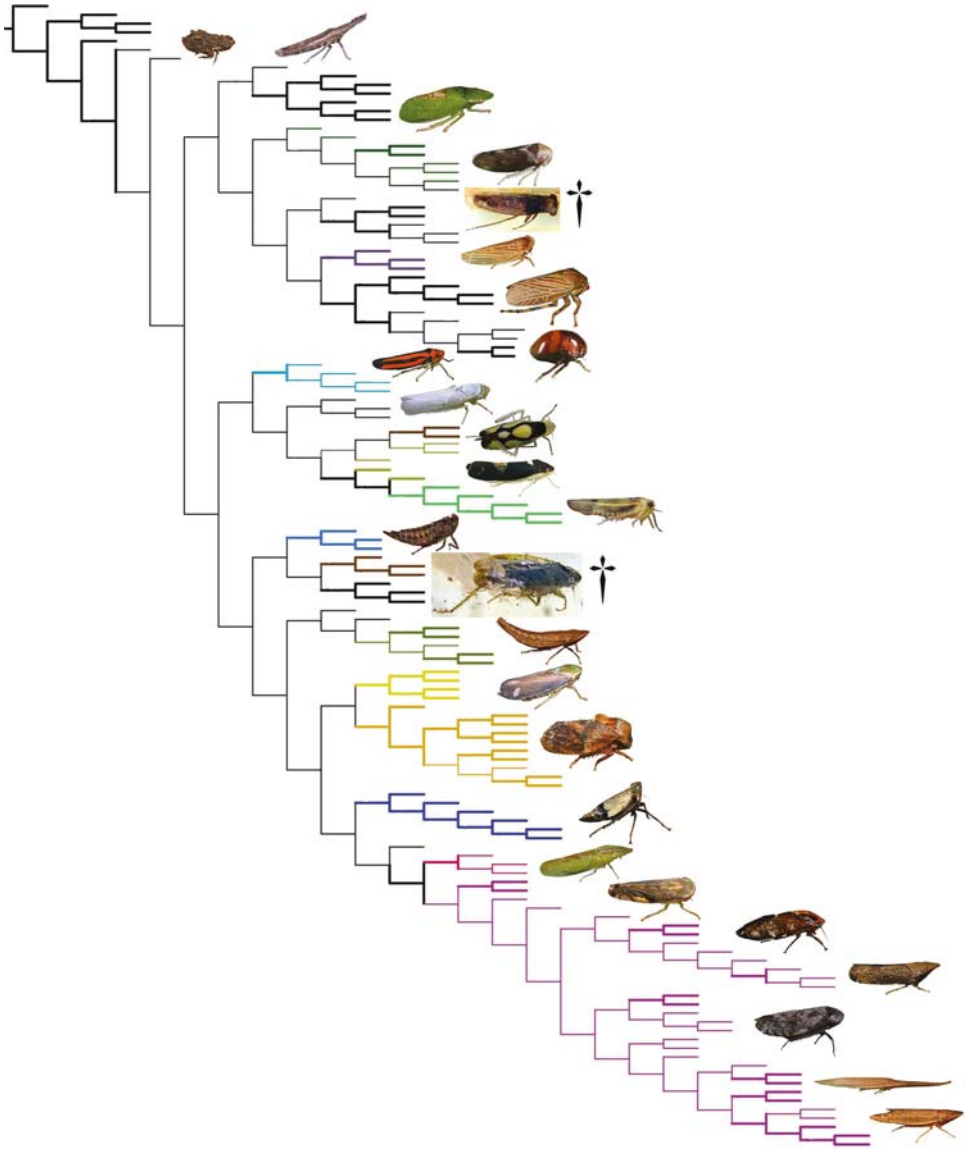

Key words: morphology, phylogeny, paleontology, Cretaceous, Eocene

Leafhoppers (Cicadellidae) are presently among the most common and abundant groups of insects. They are distributed worldwide in all terrestrial ecosystems where they feed on the vascular fluids or mesophyll cell contents of a wide variety of plants. The extant cicadellid fauna includes >23,000 named species currently grouped into 19 subfamilies (Dietrich 2005, Zahniser and Dietrich 2013, Dietrich and Thomas 2018, Xue et al. 2020). Phylogenetic studies have begun to elucidate relationships among major lineages of leafhoppers (Dietrich et al. 2001, 2017) but efforts to estimate the times of origin of these lineages have been hampered by the extremely sparse and fragmentary fossil record of the group (Dietrich and Gonçalves 2014, Dietrich and Thomas 2018, Chen et al. 2021).

Although leafhopper-like insects (superfamily Membracoidea) of the extinct family Archijassidae are recorded from as early as the Triassic (>220 Mya; Shcherbakov 1992, 2012), true leafhoppers (Cicadellidae) do not appear in the fossil record until the Lower Cretaceous (Aptian), represented by rock fossils from Brazil (~125 Ma; Hamilton 1990), Australia (~118 Ma; Hamilton 1992) and China (~125 Ma; Zhang 1997). These fossils are mostly either too poorly preserved or morphologically generalized and lacking characters that would allow them to be placed with confidence in any modern subfamily.

Recent molecular phylogenetic studies of leafhoppers have attempted to estimate the ages of various cicadellid groups by calibrating the ages of a few lineages using available fossils from the Eocene and Miocene (Baltic and Dominican amber inclusions) and the root node based on the oldest known Cicadellidae from the Lower Cretaceous (Krishnankutty 2012, Catanach 2013, Krishnankutty et al. 2016, Dietrich et al. 2017, Wang et al. 2017, Cao et al. 2022). These studies have consistently suggested that the 19 recognized modern leafhopper subfamilies arose during the Cretaceous. Until now, however, the only modern subfamilies recorded from this

period are Ledrinae (Hamilton 1990, Shcherbakov 1992, Chen et al. 2019a), Signoretiinae (Poinar and Brown 2020, Dietrich and Thomas 2018) and Coelidiinae (Wang et al. 2019). The latter two groups, along with *Qilia regilla* Chen et al. (2019a, Ledrinae) and the related *Duyana* (Chen et al. 2021) were, until now, the only adult leafhoppers recorded from Cretaceous-age amber, all from mid-Cretaceous (lower Cenomanian) Myanmar amber with an estimated age of ~98 Ma.

Several morphology-based phylogenies depicting relationships among major lineages of leafhoppers and treehoppers (Membracoidea) have been published over the past four decades (Hamilton 1983, Dietrich and Deitz 1993, Dietrich 1999, Dietrich et al. 2001, 2005, 2010). Some more recent phylogenetic studies of individual membracoid lineages have combined molecular and morphological data (Zahniser and Dietrich 2010, Krishnankutty et al. 2016, Wang et al. 2017, Xue et al. 2020). However, so far, only one membracoid fossil (an undescribed aetalionid from Dominican amber) has ever been incorporated into an explicit phylogenetic analysis (Dietrich and Deitz 1993). Also, the previous morphology-based phylogenies examining relationships among all major lineages of leafhoppers and treehoppers (Dietrich 1999; Dietrich et al. 2005, 2010) were published as conference proceedings and did not include the original data matrices or character lists, although many of the characters were incorporated into an online interactive key to subfamilies and tribes (Dmitriev 2003).

Recent discoveries of Cretaceous and Paleogene leafhoppers preserved in amber provide the first opportunity to record the states of many morphological characters, such as leg structure and chaetotaxy, crucial for placing these taxa within the modern higher classification of the family and for elucidating their phylogenetic relationships through explicit cladistic analysis. Here we describe additional leafhopper taxa from Cretaceous Myanmar amber: seven adults belonging to three extinct genera representing a new subfamily. We conduct morphology-based phylogenetic analyses incorporating these and some other recently described fossil taxa into the data matrix previously developed for the analysis of Dietrich et al. (2010). This data matrix includes representatives of all major extant membracoid lineages in order to elucidate relationships of fossil taxa to modern leafhoppers and facilitate their use for calibrating node ages in future molecular divergence time analyses.

Materials and Methods

Fossil Specimens

Cretaceous age fossils described herein originated from mines in the Hukawng Valley, Kachin, Myanmar. The age of this amber fauna has been estimated at ~98 Ma (Early Cenomanian; Shi et al. 2012). Specimens examined were purchased from a dealer in Yunnan Province, China, in 2017 by the last author and are deposited in the insect collection of Northwest A&F University, Yangling, Shaanxi, China (NWAFU), except for one specimen (the holotype of *Burmotettix brunnescens* sp. nov., described below) purchased from a dealer in Italy in 2017 by the senior author and deposited in the Illinois Natural History Survey Fossil Insect Collection, Prairie Research Institute Center for Paleontology, Champaign, Illinois, USA (INHS). We acknowledge recent ethical concerns regarding research on amber obtained from Myanmar (e.g., Engel 2020) but also note that the U.N. Human Rights Council has not recommended a ban on trade in amber from Myanmar and that amber mining and cutting continue to represent important income sources for local people (Peretti 2021). To the extent possible, we have followed the recommendations of the International Society of Palaeoentomology (Szwedo et al. 2020).

Amber specimens were prepared according to the protocols described by Nascimbene and Silverstein (2000) and Bisulca et al. (2012). Photomicrographs were taken using an AxioCam HRc Rev. 3 attached to a Zeiss SteREO Discovery.V20 zoom stereomicroscope with Plan-Apochromat S 0.63 × FWD 81 mm and Plan-Apochromat S 1.5 × FWD 30 mm objectives. All measurements were taken with the Zen 2 (Blue edition) software. Images were stacked using Helicon Focus 6, and mosaics were assembled in Adobe Photoshop CC.

Drawings were prepared by tracing over photographs. For bilaterally symmetrical parts of the head and thorax obscured by flaws in the amber or distorted due to shrinkage, drawings were prepared by tracing one half (the fully visible side) and reconstructing the other half using its mirror image.

Taxon Sample and Morphological Characters

Representatives of each cicadellid subfamily were selected based on material available in the collections of the Illinois Natural History Survey (Table 1). Preference was given to taxa for which specimens were available both for DNA extraction and morphological study. Larger subfamilies were represented by multiple tribes, genera, and species. An effort was made to choose exemplars spanning the morphological variation present in the various subfamilies. Nevertheless, much variation is not captured in the present data set and more detailed analyses will be needed to fully elucidate the extent to which the selected characters vary within each group. An effort was also made to include some taxonomically problematic genera to help elucidate their relationships to better known groups. Special effort was made to include characters that might help clarify the relationships of such taxa. Morphological terminology follows Dietrich (2005) except wing venation (Fig. 8d and e), which is slightly modified from Emeljanov (1987).

Scored fossil taxa include the three new genera described from Myanmar amber fossils below. Two of the genera, *Kachinella* Dietrich and Zhang, gen. nov. and *Viraktamathus* Dietrich and Zhang, gen. nov., are known from single female individuals. The third genus, *Burmotettix* Dietrich and Zhang, gen. nov., is known from five specimens, including males and females representing different species. To the extent that variation could be assessed among available specimens, given their different states of preservation, all of the included characters appeared to be invariant among *Burmotettix* species except for those of the abdominal terminalia specific to a single sex. Thus, the single OTU included for this taxon is a chimera combining observations from multiple specimens in order to maximize the character information available for the genus. In addition to the taxa described below, we scored morphology of the Myanmar amber fossil taxa *Priscacutius denticulatus* (Poinar and Brown 2020) and *Qilia regilla* (Chen et al. 2019a) based on information provided in the original published descriptions and illustrations. A more recently described representative of Ledrinae also from Myanmar amber (*Duyana electronica* Chen et al. 2021) was not included but appears to be identical to *Qilia* for the morphological characters included in our data matrix, differing mainly in minor details of the head and pronotal structure and forewing venation. We also scored the peculiar Eocene Baltic amber fossil *Eomegophthalmus lithuaniensis* (Dietrich and Gonçalves 2014) by examining the holotype deposited at INHS.

Outgroups were selected from other superfamilies of Auchenorrhyncha (Cicadoidea, Cercopoidea, and Fulgoroidea).

Table 1. Taxa scored for cicadellid morphological data matrix

Famly/subfamily	Tribe	Species	Locality
Outgroup			
CICADIDAE		*Cicadetta calliope*	Illinois
CERCOPIDAE		*Prosapia bicincta*	Illinois
CLASTOPTERIDAE		*Clastoptera obtusa*	Illinois
Ingroup			
MYERSLOPIIDAE		*Mapuchea* sp.	Chile
AETALIONIDAE	Aetalionini	*Aetalion nervosopunctatum*	Arizona
MELIZODERIDAE	Melizoderini	*Llanquihuea pilosa*	Chile
MEMBRACIDAE	Endoiastini	*Endoiastus* sp.	Ecuador
MEMBRACIDAE	Microcentrini	*Microcentrus perditus*	Illinois
MEMBRACIDAE	Membracini	*Campylenchia latipes*	Illinois
MEMBRACIDAE	Terentiini	*Cereon vitta*	Australia
MEMBRACIDAE	Acutalini	*Euritea munda*	Mexico
MEMBRACIDAE	Ceresini	*Poppea evelyna*	Mexico
MEMBRACIDAE	Polyglyptini	*Publilia concava*	Illinois
MEMBRACIDAE	Micrutalini	*Trachytalis isabellina*	Mexico
CICADELLIDAE			
Aphrodinae	Aphrodini	*Anoscopus serratulae*	Illinois
Aphrodinae	Aphrodini	*Aphrodes bicincta*	Illinois
Aphrodinae	Euacanthellini	*Euacanthella palustris*	Australia
Aphrodinae	Portanini	*Portanus* sp.	Ecuador
Aphrodinae	Sagmatiini	*Paulianiana dracula*	Madagascar
Aphrodinae	Xestocephalinae	*Xestocephalus desertorum*	Illinois
Bathysmatophorinae	Bathysmatophorini	*Bathysmatophorus shabliovskii*	Russia
Bathysmatophorinae	Bathysmatophorini	*Hylaius oregonensis*	Oregon
Bathysmatophorinae	Bathysmatophorini	*Lystridea uhleri*	California
†Burmotettiginae	Burmotettigini	*Burmotettix* spp.	Myanmar
†Burmotettiginae	Burmotettigini	*Kachinella bicolor*	Myanmar
†Burmotettiginae	Burmotettigini	*Viraktamathus burmensis*	Myanmar
Cicadellinae	Cicadellini	*Cicadella viridis*	Kyrgyzstan
Cicadellinae	Phereurhinini	*Clydacha ballista*	Peru
Cicadellinae	Proconiini	*Homalodisca lacerta*	California
Cicadellinae	Proconiini	*Paraulacizes irrorata*	Illinois
Cicadellinae	Tungurahualini	*Ilyapa viridis*	Peru
Cicadellinae	Tungurahualini	*Tungurahuala* sp.	Colombia
Coelidiinae	Coelidiini	*Coelidia* sp.	Ecuador
Coelidiinae	Equeefini	*Equeefa castelnaui*	South Africa
Coelidiinae	Teruliini	*Jikradia olitoria*	Illinois
Coelidiinae	Tinobregmini	*Tinobregmus viridescens*	Illinois
Coelidiinae	Youngolidiini	*Youngolidia* sp.	Ecuador
Deltocephalinae	Acinopterini	*Acinopterus acuminatus*	Illinois
Deltocephalinae	Acostemmini	*Acostemma* sp.	Madagascar
Deltocephalinae	Acostemmini	*Ikelebeloha cristata*	Madagascar
Deltocephalinae	Arrugadini	*Arrugada affinis*	Peru
Deltocephalinae	Athysanini	*Athysanus argentarius*	Illinois
Deltocephalinae	Chiasmini	*Exitianus exitiosus*	Illinois
Deltocephalinae	Cicadulini	*Cicadula smithi*	Illinois

Table 1. Continued

Famly/subfamily	Tribe	Species	Locality
Deltocephalinae	Cochlorhinini	*Cochlorhinus pluto*	California
Deltocephalinae	Deltocephalini	*Endria inimica*	Illinois
Deltocephalinae	Drabescini	*Drabescus* sp.	Nigeria
Deltocephalinae	Drabescini	*Parabolopona* sp.	Taiwan
Deltocephalinae	Drakensbergenini	*Drakensbergena* sp.	South Africa
Deltocephalinae	Eupelicini	*Eupelix cuspidata*	Kyrgyzstan
Deltocephalinae	Fieberiellini	*Fieberiella flori*	Illinois
Deltocephalinae	Hecalini	*Hecalus viridis*	Illinois
Deltocephalinae	Koebeliini	*Koebelia grossa*	California
Deltocephalinae	Koebeliini	*Grypotes puncticollis*	Pennsylvania
Deltocephalinae	Luheriini	*Luheria constricta*	Argentina
Deltocephalinae	Macrostelini	*Balclutha neglecta*	Illinois
Deltocephalinae	Mukariini	*Mukaria* sp.	India
Deltocephalinae	Occinirvanini	*Occinirvana eborea*	Australia
Deltocephalinae	Opsiini	*Opsius stactogalus*	Illinois
Deltocephalinae	Paradorydiini	*Paradorydium lanceolatum*	Kyrgyzstan
Deltocephalinae	Paralimnini	*Paralimnus nigritus*	Kyrgyzstan
Deltocephalinae	Penthimiini	*Penthimia americana*	Illinois
Deltocephalinae	Platymetopiini	*Platymetopius vitellinus*	Illinois
Deltocephalinae	Selenocephalini	*Selenocephalus obsoletus*	Greece
Deltocephalinae	Stegelytrini	*Placidellus* sp.	Thailand
Deltocephalinae	Stenometopiini	*Stirellus bicolor*	Illinois
Deltocephalinae	Bahitini	*Kinrentius bispinosus*	Peru
Eurymelinae	Austroagalloidini	*Austroagalloides rosea*	Australia
Eurymelinae	Eurymelini	*Eurymela distincta*	Australia
Eurymelinae	Eurymelini	*Katipo rubrivenosa*	Australia
Eurymelinae	Idiocerini	*Idiocerus pallidus*	Illinois
Eurymelinae	Idiocerini	*Rhytidodus decimusquartus*	Illinois
Eurymelinae	Balocerini	*Zaletta nereias*	Australia
Evacanthinae	Evacanthini	*Evacanthus nigramericanus*	Illinois
Evacanthinae	Nirvanini	*Nirvana adelaideae*	Australia
Evacanthinae	Nirvanini	*Tahura recurvata*	Peru
Evacanthinae	Pagaroniini	*Pagaronia confusa*	California
Evacanthinae	Pagaroniini	*Friscanus friscanus*	California
Hylicinae	Hylicini	*Hatigoria sauteri*	Taiwan
Iassinae	Bythoniini	*Bythonia* sp.	Ecuador
Iassinae	Iassini	*Batracomorphus irroratus*	Kyrgyzstan
Iassinae	Iassini	*Penestragania robusta*	Illinois
Iassinae	Iassini	*Platyhynna* sp.	Peru
Iassinae	Krisnini	*Krisna gravis*	Nigeria
Iassinae	Scarini	*Gyponana panda*	Illinois
Iassinae	Scarini	*Scaris* sp.	Peru
Iassinae	Selenomorphini	*Selenomorphus* sp.	New Caledonia
Iassinae	Trocnadini	*Trocnada dorsigera*	Australia
Iassinae	unplaced	*Scaroidana flavida*	Argentina
Ledrinae	Afrorubrini	*Afrorubria* sp.	South Africa

Table 1. Continued

Famly/subfamily	Tribe	Species	Locality
Ledrinae	Ledrini	*Ledra* sp.	Taiwan
Ledrinae	Ledrini	*Petalocephala* sp.	Taiwan
Ledrinae	Xerophloeini	*Proranus adspersipennis*	Venezuela
Ledrinae	Xerophloeini	*Xedreota* sp.	Ecuador
Ledrinae	Xerophloeini	*Xerophloea peltata*	Illinois
Ledrinae	Paracarsonini	*Qilia regilla*	Myanmar
Macropsinae	Macropsini	*Macropsis ferrugineoides*	Illinois
Megophthalminae	Adelungiini	*Platyproctus maculipennis*	Israel
Megophthalminae	Agalliini	*Aceratagallia uhleri*	Illinois
Megophthalminae	Megophthalmini	*Brenda* sp.	Mexico
Megophthalminae	Megophthalmini	*Tiaja friscana*	California
Megophthalminae	Evansiolini	*Evansiola insularis*	Chile
†Megophthalminae	unplaced	*Eomegophthalmus*	Baltic amber
Mileewinae	Makilingiini	*Makilingia* sp.	Philippines
Mileewinae	Mileewini	*Amahuaka* sp.	Mexico
Mileewinae	Tinteromini	*Tinteromus* sp.	Peru
Neobalinae	Neobalini	*Calliscarta* sp.	Ecuador
Neobalinae	Neobalini	*Chibala modesta*	Chile
Neocoelidiinae	Macroceratogoniini	*Macroceratogonia* sp.	New Caledonia
Neocoelidiinae	Neocoelidiini	*Biza* sp.	Ecuador
Neocoelidiinae	Neocoelidiini	*Chinaia* sp.	Ecuador
Neocoelidiinae	Neocoelidiini	*Neocoelidia tumidifrons*	Illinois
Nioniinae	Nioniini	*Nionia palmeri*	Illinois
Signoretiinae	Phlogisini	*Phlogis* sp.	Malaysia
Signoretiinae	Signoretiini	*Signoretia* sp.,	Nigeria
Tartessinae	Neopsini	*Neopsis* sp.	Peru
Tartessinae	Stenocotini	*Stenocotis depressa*	Australia
Tartessinae	Tartessini	*Tartessoides griseus*	Australia
Tartessinae	Thymbrini	*Putoniessa* sp.	Australia
Typhlocybinae	Alebrini	*Alebra aurea*	Illinois
Typhlocybinae	Dikraneurini	*Dikraneura angustata*	Illinois
Typhlocybinae	Empoascini	*Empoasca fabae*	Illinois
Typhlocybinae	Erythroneurini	*Erasmoneura vulnerata*	Illinois
Typhlocybinae	Forcipatini	*Forcipata loca*	Illinois
Typhlocybinae	Typhlocybini	*Typhlocyba querci*	Illinois
Ulopinae	Cephalelini	*Paracephaleus brunneus*	Australia
Ulopinae	Coloborrhinini	*Coloborrhis corticina*	South Africa
Ulopinae	Ulopini	*Ulopa reticulata*	U.K.
unplaced		LH 178	Ecuador

Fossil taxa are indicated by '†'.

Discrete morphological character data were scored by the first author and added to a data matrix for Membracoidea originally compiled by Dietrich (1999) and subsequently expanded by adding more characters and taxa comprising representatives of all presently recognized subfamilies of Membracoidea (Dietrich et al. 2005, 2010). Morphological terminology, characters, and states generally follow Dietrich (2005) and are illustrated in Figs. 8–13. Characters were scored based on original observations of specimens of exemplar taxa. Because nymphs of many of the exemplar species were not available for study, character states were, in some cases, inferred based on study of other taxa belonging to the same tribe. If no exemplar from a particular tribe or subfamily was available, the nymphal characters of the included exemplar were scored as missing values.

The following morphological characters were scored for each taxon. Character states are illustrated in Figs. 8–13 unless otherwise noted. The data matrix is given in Supp Table S1 (online only).

Head

1. Rostrum length: 0, not surpassing front trochanters; 1, extended well beyond front trochanters.
2. Distal segment of rostrum length: 0, little if any longer than penultimate segment (Fig. 8b); 1, nearly 2× longer than penultimate segment (Fig. 9a).
3. Anteclypeus convexity: 0, strongly inflated (Fig. 9d); 1, convex but not inflated (maximum depth less than half width); 2, flat or very slightly convex (Fig. 9i).
4. Anteclypeus shape in anterior view: 0, tapered distally (Fig. 9b); 1, more or less parallel (may be slightly narrower at base or apex than at midlength; Fig. 9n); 2, constricted, narrowest near base (Fig. 9a). This character tends to vary among tribes within subfamilies, but is relatively stable within tribes and has been used to distinguish tribes of Deltocephalinae (e.g., Hamilton 1975).
5. Anteclypeus length: 0, less than 2.5× basal width; 1, ~3× basal width.
6. Anteclypeus transverse preapical fold: 0, absent; 1, present.
7. Anteclypeus apex extension: 0, not extended to apex of maxillary plate (Fig. 9h); 1, even with maxillary plate; 2, extended beyond maxillary plate (Fig. 9b).
8. Clypeal suture: 0, complete; 1, incomplete, obsolete medially (Fig. 9n).
9. Maxillary (subgenal) suture or emargination: 0, absent; 1, present as suture only (Fig. 9j); 2, present as distinct cleft (Fig. 9f). State 2 appears to be restricted to Ulopinae; state one, which may be homologous, occurs in treehoppers and in some Megophthalminae, but in the latter group, the suture is very weakly developed or absent.
10. Maxillary sensillum position: 0, dorsad or even with clypeal suture (Fig. 9l); 1, distinctly ventrad of clypeal suture, near lorum; 2, ventrad of clypeal suture distant from lorum; 3, on or very near ventral margin of maxillary plate; 4, on lateral or posterior surface of maxillary plate; 5, absent.
11. Erect fine seta on gena below antennal pit: 0, absent (recumbent setae may be present); 1, present (Fig. 9e).
12. Gena, shape: 0, narrow, strongly emarginate below eye (Fig. 9f); 1, more or less evenly rounded (Fig. 9l); 2, subangulately produced ventrolaterally (Fig. 9e).
13. Lorum size: 0, narrow, elongate, length more than 2× width (Fig. 9k); 1, length approximately 2× width; 2, broad, length distinctly less than 2× width.
14. Lorum shape: 0, flat; 1, distinctly convex.
15. Lorum distance from maxillary plate margin: 0, extended to or narrowly separated from margin (Fig. 9i); 1, distant from margin (Fig. 9k).
16. Subgenal suture extension: 0, extended to or very near clypeogenal suture dorsally; 1, terminating some distance from clypeogenal suture dorsally.
17. Portion of lorum bordering frontoclypeus: 0, more than half; 1, between 1/3 and 1/2; 2, less than 1/3; 3, lorum entirely bordering anteclypeus (Fig. 9k).
18. Face texture: 0, not or only finely punctate; 1, coarsely punctate dorsally; 2, with coarse punctation arranged in arcuate series (Fig. 9o).
19. Epistomal suture: 0, not visible or poorly delimited; 1, distinct, sulcate (outgroups).
20. Frontoclypeus proportions: 0, maximum width equal to or greater than length; 1, maximum width less than length.
21. Frontoclypeus distance from eye: 0, less than postclypeus maximum width; 1, greater than postclypeus maximum width (Fig. 9b).
22. Frontoclypeus median longitudinal carina: 0, absent; 1, present.
23. Frontoclypeus median carina development: 0, complete (Fig. 9l); 1, incomplete (Fig. 9k). This character is scored as? for taxa lacking a median carina.
24. Frontoclypeus lateral carina adjacent to antennal base: 0, absent; 1, present below antennal pit (Fig. 9i).
25. Frontoclypeus transverse median ridge: 0, absent; 1, present.
26. Facial sutures, position relative to ocelli: 0, extended ventromesad of ocelli (temporal suture obsolete; Fig. 9i); 1, extended both mesad and laterad of ocelli (temporal and epistomal sutures distinct; Fig. 9d); 2, extended laterad of ocelli (epistomal suture obsolete).
27. Laterofrontal suture, length: 0, extended to or near ocellus (Fig. 9n); 1, ended abruptly a short distance dorsad of antennal ledge (Fig. 9c); 2, absent (or indicated only by pigment; Fig. 9j).
28. Anterior tentorial arm: 0, absent; 1, present, connecting tentorial bridge to anterior tentorium (outgroups).
29. Crown texture: 0, same as that of face; 1, distinctly different from that of face, at least posteriorly.
30. Crown anterior margin, transverse parallel grooves or carinae: 0, absent; 1, present.
31. Crown transverse carinae number: 0, numerous, irregular; 1, few, parallel (Fig. 9e). Taxa without transverse grooves or carinae are scored as ? for this character.
32. Crown anterior margin shape in profile: 0, rounded to face; 1, distinctly carinate.
33. Crown lateral margin orientation: 0, parallel to midline; 1, divergent from midline anteriorly.
34. Coronal suture: 0, not visible; 1, present but not extended beyond midlength of crown; 2, extended well anterad of crown midlength (Fig. 9l).
35. Crown longitudinal carina: 0, absent; 1, present anteriorly (on acrometope); 2, present posteriorly (on coryphe); 3, extended throughout length (Fig. 9l).
36. Crown, numerous oblique lateral carinae, convergent toward apex: 0, absent; 1, present (Fig. 9l).
37. Crown lateral margins elevation: 0, not or only gradually elevated; 1, abruptly elevated and ledge-like adjacent to eyes (sometimes only in nymphs; Fig. 9m).
38. Crown median length relative to length next to eyes: 0, shorter medially than adjacent to eyes (Fig. 9p); 1, subequal; 2, distinctly longer medially (Fig. 9q).
39. Anterior tentorium shape: 0, linear or weakly curved; 1, apex weakly bilobed and curved, falcate; 2, apex distinctly bilobed or bifurcate; 3, greatly reduced or absent.
40. Crown width: 0, greater than or equal to 1.5× eye width; 1, less than 1.5× eye width
41. Crown posterolateral extensions: 0, absent, crown not or only slightly extended posterad of eye; 1, well developed, crown distinctly extended posterolaterad of eye for greater than half eye width (Fig. 9q).
42. Eye mesal margin: 0, entire; 1, distinctly emarginate adjacent to antennal base (Fig. 9i); 2, emarginate adjacent to crown margin (crown apparently overlapping eye).
43. Antennal ledge aspect: 0, weakly or not encroaching onto frontoclypeus; 1, strongly encroaching onto frontoclypeus (state 1 occurs in Myerslopiidae and outgroups; Hamilton 1999).

44. Antennal ledge shape in anterior view: 0, curved and depressed, covering antennal base in anterior view (Fig. 9f); 1, curved and digitiform (Fig. 9m); 2, present only as carina (Fig. 9e); 3, absent.
45. Antennal ledge shape in dorsal view: 0, not prominent, forming continuous curve with crown margin; 1, distinctly projecting beyond curve of crown margin (Fig. 9q).
46. Antennal pit position: 0, near anteroventral corner of eye (Fig. 9l); 1, near mid-height of eye; 2, near anterodorsal corner of eye (Fig. 9k).
47. Antennal flagellum aspect: 0, not annulate; 1, annulate.
48. Flagellum length: 0, shorter than head width; 1, longer than head width, but less than half body length; 2, more than half body length.
49. Frontoclypeus extension: 0, entirely on face (Fig. 9j); 1, extended to or posterodorsad of crown margin (Fig. 9d). This character is difficult to score for some groups because the epistomal suture and the muscle scars of the cibarial dilators are often reduced or absent.
50. Median ocellus: 0, absent; 1, present.
51. Ocelli (or ocellar vestiges), position relative to anterior margin of head: 0, on crown, distant from anterior margin and eyes (Fig. 9d); 1, on crown, slightly posterad of anterior margin or in marginal grooves, and distant from eyes (Fig. 9h); 2, on anterior margin (Fig. 9e); 3, on face distinctly below margin of crown (Fig. 9j).
52. Ocelli, position relative to antennal pits: 0, distinctly mesad (lfs convergent; Fig. 9j); 1, approximately even with or laterad (lfs parallel or divergent; Fig. 9e).
53. Ocelli position relative to ecdysial line (frontal suture): 0, less than one diameter distant (Fig. 9g); 1, ca. one diameter distant; 2, more than one diameter distant (Fig. 9f).
54. Ocelli, development: 0, well developed, prominent and distinctly convex; 1, well developed, small, not prominent; 2, vestigial or absent.

Thorax

Pronotum

55. Anterior margin projection: 0, not produced anterad of eyes; 1, strongly produced and subangulate, anterior margin even with or exceeding anterior margins of eyes (Fig. 9p).
56. Posterior margin extension: 0, not extended to scutellum (Fig. 9p); 1, extended to or overlapping scutellum (Fig. 9q).
57. Posterior process: 0, absent; 1, well developed, overlapping, and partially or completely concealing scutellum in dorsal view.
58. Lateral margin length: 0, short, eye nearly touching forewing base; 1, 0.5–1.0× eye width (Fig. 9m); 2, greater than 1.0× eye width.
59. Lateral carina, position of anterior end relative to eye: 0, even with or above posterior corner of eye (Fig. 9m); 1, ventrad of posterior corner of eye.
60. Transverse striations: 0, absent or indistinct; 1, well developed across entire length of pronotum.
61. Setigerous tubercles: 0, absent; 1, present.

Other Sclerites

62. Proepisternum size (best seen with head removed): 0, large, exposed, not lamelliform (Fig. 9m); 1, small, poorly developed; 2, well-developed, lamelliform.
63. Proepisternum exposure: 0, mostly exposed (Fig. 9m); 1, mostly concealed by gena (Fig. 9i).
64. Mesonotum: 0, without parapsidal clefts (only sutures present; Fig. 9u); 1, with parapsidal clefts; Fig. 9t).
65. Scutellum surface: 0, flat; 1, with median longitudinal ridge or keel.
66. Mesepisternum division: 0, divided into anepisternum and katepisternum; 1, not divided, forming a single continuous sclerite.
67. Mesanepisternum aspect: 0, normal; 1, produced and carinate below wing at rest, shelflike (Fig. 9r).
68. Mesepisternal hook: 0, absent; 1, present (Fig. 9s).
69. Meskatepisternum digitiform process: 0, absent; 1, present (Fig. 9r).

Forewing

70. Development: 0, macropterous; 1, submacropterous or brachypterous (Fig. 10c); 2, elytralike (hindwing vestigial; Fig. 10b). Although most groups assigned state 1 have macropterous forms, these tend to be rare.
71. Shape: 0, ovoid, broadened to midlength, thence narrowed to rounded apex; 1, triangular, broadened from base to near apex, apex obliquely truncate and forming angle with commissural margin.
72. Membrane texture: 0, glabrous; 1, densely microtrichiose (shagreen).
73. Membrane vestiture: 0, without setae; 1, with setae or scales, not associated with pits; 2, with setae associated with distinct pits.
74. Veins elevation: 0, not distinctly elevated or carinate; 1, distinctly elevated and carinate.
75. Veins setation: 0, without conspicuous setae; 1, conspicuously setose.
76. Veins R and M fusion: 0, forming common stem near base, Cu free (Fig. 10a); 1, M united with Cu near base, R free (Fig. 10d).
77. Vein R branches: 0, with two branches (Fig. 10j); 1, with three or more branches (not including supranumerary veinlets) distad of fork. Intratribal variation in this character occurs in Eurymelinae and Megophthalminae. Score as missing if brachypterous.
78. RA_1 origin: 0, arising directly from R stem (Fig. 10d); 1, arising distad of RP fork.
79. RA_1 location: 0, closer to RP fork than to s crossvein (Fig. 10a); 1, closer to s-crossvein (Fig. 10g). Taxa scored as state 0 for character 73 are scored as? for this character.
80. RA_2 shape: 0, straight or weakly recurved (Fig. 10a); 1, strongly recurved, forming more or less continuous line with crossvein s (Fig. 10h).
81. Crossvein s (=r or ir of authors): 0, absent; 1, present or RA2 and RP confluent (Fig. 10a).
82. Crossvein r-m_1: 0, absent; 1, present (Fig. 10a).
83. Veins RP and MA fusion: 0, free; 1, confluent preapically (Fig. 10j).
84. Crossvein m-cu_2: 0, absent; 1, present.
85. Crossvein m-cu_2 connection: 0, connected to Cu basad of fork (Fig. 10a); 1, connected to m-cu_3 (Fig. 10e).
86. CuA: 0, connected to submarginal vein at claval apex (Fig. 10d); 1, connected to submarginal vein well distad of claval apex (Fig. 10l).
87. Inner apical cell shape: 0, short, broad, tapered distally, not parallel to anal margin (Fig. 10h); 1, narrow, elongate, parallel to anal margin (Fig. 10i).
88. Inner apical cell base shape: 0, with lateral corner basad of mesal corner (Fig. 10l); 1, with lateral corner even with or distad of mesal corner (Fig. 10i).

89. Inner apical cell width: 0, as wide as or wider than other cells, apex oblique or rounded, not acuminate; 1, narrow and acuminate apically (Fig. 10m).
90. Inner apical cell texture: 0, same as that of adjacent cells; 1, distinctly different from that of adjacent cells (membranous, unpigmented).
91. Brachial cell shape: 0, parallel sided through most of length; 1, distinctly widened from base to apex, broader at base of apical cell than at midlength.
92. Clavus (shape): 0, acuminate, apex acute or narrow and blunt (Fig. 10a); 1, broadly truncate or rounded apically (Fig. 10d).
93. Clavus (crossveins): 0, without crossveins; 1, with crossvein between vein Pcu and claval suture and/or between veins Pcu and A1 (Fig. 10k).
94. Appendix: 0, absent (Fig. 10j); 1, restricted to anal margin (Fig. 10h); 2, extended around wing apex (Fig. 10e).

Hind Wing

95. Costal margin subbasal lobe: 0, without broad subbasal lobe; 1, with broad subbasal lobe (Fig. 10o).
96. Hind wing apex texture: 0, glabrous or minutely granulose; 1, with semicircular chaetoids.
97. Apical margin: 0, entire; 1, emarginate.
98. RA2 (costal portion of submarginal vein): 0, complete (Fig. 10p); 1, incomplete, not reaching RP or R+M; 2, absent (Fig. 10s).
99. Submarginal vein position: 0, well separated from apical margin (Fig. 10p); 1, near or coincident with margin apically.
100. Submarginal vein extension: 0, complete at wing apex between apices of RP (or R+M) and MP; 1, absent or greatly reduced (Fig. 10q).
101. Submarginal vein extension: 0, not extended onto jugum; 1, extended onto jugum (Fig. 10r).
102. RP and MA fusion: 0, free; 1, confluent preapically (Fig. 10n).
103. Crossvein m-cu length: 0, long, subequal to or longer than basal segment of MP (Fig. 10o); 1, less than half as long as basal segment of MP (Fig. 10p); 2, absent, MP and CuA confluent preapically.
104. Crossvein m-cu orientation: 0, forming oblique angle with MP and CuA (Fig. 10o); 1, perpendicular to MP and CuA, or nearly so (Fig. 10p).
105. Pcu and A1 fusion: 0, separate distally; 1, completely fused (Fig. 10t).
106. Base of vein MP sclerotization: 0, well sclerotized; 1, distinctly less sclerotized than other veins.

Legs

107. Prothoracic femur, row AM development: 0, with several macrosetae (Fig. 11a); 1, with only AM1; 2, absent or undifferentiated.
108. Prothoracic femur AM1 position: 0, near middle of anterior tibial surface (Fig. 11b); 1, on or near anteroventral margin (Fig. 11d).
109. Prothoracic femur, row AV development: 0, more or less continuous from base to apex; 1, restricted to distal half; 2, only AV1 present (Fig. 11d); 3, only basal half and AV1 present (Fig. 11a); 4, absent or indistinct; 5, with very short, stout seta near 2/3 length (Fig. 11e).
110. Prothoracic femur, row AV-B (basal group of anteroventral row) setae development: 0, undifferentiated or long and widely spaced; 1, shorter and stouter than other ventral setae (Fig. 11a); 2, with few long, evenly spaced macrosetae; 3, with a single stout macroseta near midlength (Fig. 11c).
111. Prothoracic femur, AV1: 0, undifferentiated; 1, large, stout (Fig. 11d).
112. Pro- and/or mesothoracic femur, row PV development: 0, absent; 1, with several setae (Fig. 11f); 2, only PV1 present.
113. Prothoracic femur, intercalary row (pecten) development: 0, absent or undifferentiated; 1, distinct, uniseriate; 2, multiseriate with short, fine setae.
114. Prothoracic tibia shape in cross-section: 0, more or less cylindrical; 1, with dorsal surface flattened and bicarinate; 2, flattened and expanded.
115. Prothoracic tibia, accessory adlateral macrosetal row: 0, absent; 1, present, setae scattered; 2, present, uniseriate (Fig. 11o).
116. Prothoracic tibia, dorsal setal rows: 0, with approximately equal numbers of macrosetae (Fig. 11m); 1, PD with many more setae than AD (Fig. 11n).
117. Mesocoxal meron large acute process: 0, absent; 1, present.
118. Mesothoracic trochanter setae: 0, absent; 1, with group of 2–6 stout ventroapical setae; 2, with single stout ventroapical seta.
119. Mesothoracic tibia, dense ventral patch of short setae near apex: 0, absent; 1, present.
120. Hind coxal peg and socket apparatus: 0, absent; 1, present.
121. Hind coxa shape: 0, transverse; 1, conical.
122. Hind coxal meracanthus: 0, absent; 1, present.
123. Hind coxa macrosetae: 0, without one or more ventromedial macrosetae; 1, with one or more ventromedial macrosetae
124. Hind trochanter pair of close-set, stout, dorsal setae: 0, absent; 1, present (Fig. 11dd).
125. Hind femur apex macrosetae: 0, absent; 1, present.
126. Hind femur macrosetae: 0, 0–2 apical (Fig. 11l); 1, 2 + 1 (Fig. 11j); 2, 2 + 1 + 1 (Fig. 11i); 3, 2 + 2 + X (where X is one or more antepenultimate setae), second pair widely separated (Fig. 11g); 4, 2 + 2 + X, second pair close-set (Fig. 11h).
127. Hind femur macrosetae spacing: 0, normally spaced (Fig. 11g); 1, grouped at apex (Fig. 11k).
128. Hind femur length: 0, not reaching proepimeron in repose; 1, reaching or surpassing proepimeron in repose.
129. Hind tibia, shape in cross section: 0, square or trapezoidal, distance between dorsal macrosetal rows subequal to their distance to ventral rows; 1, narrowly rectangular (dorsal rows closer to each other than to ventral rows); 2, round.
130. Hind tibia setal rows: 0, without longitudinal rows of enlarged setae (outgroups); 1, with three or more longitudinal rows of enlarged setae.
131. Hind tibia row AD setal bases (maximal development): 0, unmodified; 1, cucullate (Fig. 11q); 2, strongly produced and spinelike (Fig. 11r).
132. Hind tibial row AD carina: 0, macrosetae not situated on distinct carina; 1, macrosetae situated on distinct carina.
133. Hind tibial rows PD and AD macrosetae: 0, with approximately equal numbers of macrosetae; 1, row PD with several more macrosetae than row AD (intercalary setae subequal to primary setae; Fig. 11t).
134. Hind tibia row PD development: 0, with numerous macrosetae; 1, with 0–5 macrosetae (Fig. 11u).
135. Hind tibia row PD proximal seta: 0, aligned with others; 1, closer to row II (Fig. 11s).
136. Hind tibia row PD proximal seta position: 0, even with or distad of AD1 Fig. 11s); 1, distinctly basad of AD1.
137. Hind tibia row AD intercalary setae between large macrosetae: 0, absent; 1, present (Fig. 11q).

138. Hind tibia row AD intercalary setae bases: 0, simple; 1, cucullate (Fig. 11q). Taxa having state 0 for character 137 are scored as? for this character.
139. Hind tibia macrosetae between dorsal rows: 0, absent; 1, present.
140. Hind tibia row AV extension: 0, with macrosetae present from basal third to apex (Fig. 11q); 1, macrosetae restricted to apical half (Fig. 11p).
141. Hind tibia row AV development: 0, with >7 macrosetae; 1, with 6 or fewer macrosetae.
142. Hind tibia row AV setal bases: 0, simple; 1, distinctly cucullate.
143. Hind tibia row AV in female: 0, same as in male; 1, with setae elongate and hooked.
144. Hind tibia row PV setae size: 0, with setae of uniform size, at least in basal third, becoming gradually longer distally; 1, with alternating short and long setae.
145. Hind tibia pecten arrangement: 0, with a single transverse row of spinelike setal bases (Fig. 11y); 1, with preapical and apical rows of spinelike setal bases (Fig. 11w).
146. Hind tibia apical pecten macrosetae sizes: 0, even (Fig. 11y); 1, alternating short/long (Fig. 11x).
147. Hind tibial pecten setae aspect: 0, tapered dark macrosetae; 1, platellae (pale, blunt-tipped setae; Fig. 11v); 2, fine, pale setae.
148. Tarsi: 0, without pulvilli; 1, with well developed pulvilli.
149. Aroleum: 0, absent or poorly developed; 1, well developed, pulvilliform or setiform.
150. Hind tarsomere I heel: 0, weakly developed, not extended >1/3 total length of tarsomere; 1, well developed, extended >½ length of tarsomere (Fig. 11z).
151. Hind tarsomere I enlarged dorsoapical setae: 0, absent; 1, pair of setae present (Fig. 11bb); 2, single seta present.
152. Hind tarsomere I plantar setae arrangement: 0, both rows scattered; 1, mesal row uniseriate or reduced, outer row scattered; 2, two uniseriate rows (op. cit.: Fig. 2G).
153. Hind tarsomere I AV setae aspect: 0, simple; 1, cucullate; 2, platelliform (rounded).
154. Hind tarsomere I apex shape: 0, truncate or broadly rounded; 1, acuminate (Fig. 11aa).
155. Hind tarsomere I width: 0, slender throughout; 1, distinctly broadened distally.
156. Hind tarsomere I apical platellae (rarely tapered macrosetae) number: 0, with 6 or more; 1, with 4–5 (Fig. 11z); 2, with 3; 3, with 0–2.
157. Hind tarsomere I apical setae aspect: 0, platellae; 1, spinelike macrosetae; 2, with both platellae and spinelike macrosetae (Fig. 11cc).
158. Hind tarsomere I pecten medial seta aspect: 0, tapered and darkly pigmented; 1, tapered and pale; 2, platelliform.
159. Hind tarsomere I median subapical macroseta: 0, absent; 1, present.

Abdomen

160. Tergum II medial sclerite shape: 0, triangular; 1, T-shaped with anterolateral lobes; 2, transverse, hourglass-shaped; 3, undifferentiated; 4, membranous with anterior collar. This structure appears to be variable in some subfamilies and conservative in others. States defined here are those which occur consistently in one or more subfamilies. Others are scored as?
161. Tergum I acrotergite: 0, absent; 1, present, small; 2, present, large. Removal of the abdomen often results in obliteration of this structure; thus, many taxa are scored as missing values.
162. Sternum II apodemes: 0, absent or vestigial; 1, well developed.
163. Tergum III apodemes: 0, absent or vestigial; 1, well developed.
164. Laterotergites IV–VII fusion: 0, free, well sclerotized; 1, fused to tergites, undifferentiated.
165. Female sternite VIII exposure: 0, exposed; 1, concealed in repose.
166. Epiproct fusion: 0, differentiated from tergite XI; 1, fused to tergite XI.

Female Genitalia/Terminalia

167. Ovipositor extension: 0, not or only slightly extended posteriorly beyond pygofer; 1, extended well beyond pygofer.
168. Ovipositor exposure: 0, not largely enclosed by pygofer lobes; 1, largely enclosed by pygofer lobes in repose.
169. First valvula dorsal sculpturing, form: 0, strigate (Fig. 12a); 1, areolate or reticulate (Fig. 12b); 2, granulose, papillose, maculose, or baculiform (Fig. 12c). Sculpuring often varies over the distal half of the valvula; a single species often has multiple textures grouped as indicated in the states of this character.
170. First valvifer anterior extension: 0, absent; 1, present.
171. First valvifers fusion: 0, free; 1, fused.
172. First valvula dorsal sculpturing position: 0, marginal (Fig. 12a); 1, submarginal (Fig. 12c).
173. First valvula ventroapical sculpturing extent: 0, continuous with dorsal sculpturing (Fig. 12a); 1, in separate field (Fig. 12d); 2, in distinct triangular area (Fig. 12e).
174. Second valvula distal paired blades length: 0, less than half total length (Fig. 12i); 1, more than 2/3 total length (Fig. 12g).
175. Second valvula shape: 0, broad throughout or gradually tapered (Fig. 12n); 1, distinctly broadened medially (Fig. 12j); 2, elongate and very narrow (Fig. 12l).
176. Second valvulae ventral margin shape: 0, straight or convex; 1, arcuate (Fig. 12n); 2, strongly sigmoid.
177. Second valvulae rami extension: 0, not extended posterodorsad of valvifers (Fig. 12g); 1, extended posterodorsad of valvifers (Fig. 12l).
178. Second valvulae dorsal margins symmetry: 0, symmetrical; 1, asymmetrical (Fig. 12h).
179. Second valvula dorsomedial notch: 0, absent; 1, present (Fig. 12i).
180. Second valvula serrations: 0, absent; 1, present (Fig. 12k).
181. Second valvula, numerous closely spaced teeth: 0, absent; 1, present (teeth may be serrate; Fig. 12g).
182. Second valvula, few large irregular teeth: 0, absent; 1, present (Fig. 12f).
183. Second valvulae, median dorsal tooth: 0, absent; 1, present (Fig. 12m).
184. Second valvulae ducts branching pattern: 0, without distinct fork in main channel; 1, with distinct fork in main channel (Fig. 12m).

Male Genitalia/Terminalia

185. Valve fusion: 0, free (Fig. 13d); 1, fused to pygofer (Fig. 13a).
186. Valve (extent of fusion): 0, narrowly fused to pygofer; 1, broadly fused to pygofer (Fig. 13a). Taxa with state 0 for character 185 are scored?
187. Valve posterior margin projection: 0, not, or very weakly produced (plate bases transverse; Fig. 13b); 1, roundly produced; 2, angulately produced (Fig. 13e).
188. Valve median longitudinal internal ridge: 0, absent; 1, present.
189. Valve and plates fusion: 0, free, plates movable independent of valve; 1, partially fused, plates not independently movable; 2, completely fused, suture absent or poorly delimited.

190. Tergum IX sclerotization: 0, membranous except for narrow basal band; 1, well sclerotized but shorter than tergite VIII; 2, longer than tergite VIII.
191. Pygofer basolateral oblique membranous cleft: 0, absent; 1, present.
192. Pygofer lateral plate: 0, absent; 1, present and distinctly separate from pygofer.
193. Pygofer macrosetae: 0, absent or poorly differentiated; 1, well differentiated
194. Pygofer macrosetae (number): 0, numerous; 1, fewer than 5 present on or near dorsoapical margin.
195. Pygofer dense cluster of peglike setae distally: 0, absent; 1, present (Fig. 13f).
196. Subgenital plates fusion: 0, free throughout length; 1, fused to each other, at least at base (Fig. 13b).
197. Subgenital plate macrosetae development: 0, absent or poorly differentiated; 1, well differentiated.
198. Subgenital plate macrosetae arrangement: 0, scattered (Fig. 13c); 1, uniseriate on or near lateral margin (Fig. 13e); 2, uniseriate far from lateral margin (Fig. 13k).
199. Subgenital plate fine setae: 0, absent or very sparse and inconspicuous; 1, numerous, conspicuous (Fig. 13f).
200. Subgenital plate shape: 0, ligulate, widest near or beyond midlength (Fig. 13c); 1, not ligulate, widest at or near base, or margins subparallel (Fig. 13d).
201. Subgenital plate dorsal fold articulated to style: 0, absent or restricted to base; 1, present, extended to or beyond midlength.
202. Subgenital plates and valve exposure: 0, not or only slightly retracted, at most with base of plate concealed; 1, largely retracted into 8th abdominal basal half or more of plate concealed (Fig. 13n).
203. Subgenital plate distal half shape: 0, laterally compressed (Fig. 13c and f); 1, depressed, tapered (Fig. 13a and b).
204. Subgenital plate segmentation: 0, not subsegmented; 1, subsegmented.
205. Style base shape: 0, elongate, broadened apically (Fig. 13f); 1, moderately long, tapered; 2, apodeme short, broadly bilobed, extended well anterad of connective; 3, apodeme short, broadly bilobed, extended little or no further anterad than connective (Fig. 13e).
206. Style median basal lobe development: 0, poorly developed; 1, greatly enlarged (Fig. 13e and m).
207. Style apex shape: 0, not spatulate, without median preapical tooth; 1, spatulate with median preapical tooth.
208. Style apophysis vestiture: 0, without teeth; 1, serrate or denticulate (Fig. 13m).
209. Style lateral lobe: 0, absent; 1, present, moderately developed; 2, greatly enlarged, style cheliform (Fig. 13k and m).
210. Style apophysis length: 0, elongate, longer than section of shank basad of lateral lobe (Fig. 13h); 1, as short as or shorter than section of shank basad of lateral lobe.
211. Connective: 0, not differentiated, enlarged phallobase present at base of aedeagus; 1, well differentiated, small (may be fused to aedeagus).
212. Connective anterior arms: 0, absent, very short, or strongly divergent (Fig. 13b); 1, well developed, subparallel, or convergent distally (Fig. 13m).
213. Connective median anterior lobe: 0, present (Fig. 13k); 1, absent (Fig. 13e).
214. Connective median posterodorsal keel: 0, absent, connective stem depressed; 1, present, connective stem compressed (Fig. 13j).
215. Aedeagus: 0, not differentiated into theca and endotheca; 1, differentiated into theca and endotheca (Fig. 13l).
216. Aedeagus guide: 0, absent; 1, present and well sclerotized within genital capsule (Fig. 13l).
217. Gonoduct base: 0, entirely membranous; 1, partially sclerotized, conelike (Fig. 13j).
218. Aedeagus dorsal apodeme development: 0, membranous, poorly delimited; 1, well-sclerotized, column- or platelike (Fig. 13d and e); 2, subsegmented, 'dorsal connective' present (Fig. 13g); 3, bifurcate.
219. Anal tube basolateral process: 0, absent; 1, present, rigidly attached (Fig. 13a and b); 2, present, arising from separate ringlike sclerite; 3, present, separate, articulated to pygofer; 4, present, separate, continuous with dorsal apodeme of aedeagus.
220. Anal tube dorsal sclerotization: 0, well developed; 1, incomplete or absent.
221. Anal tube ventral sclerotization: 0, absent; 1, present.

Nymphs

222. Ecdysial line in adults: 0, absent; 1, distinct (Dmitriev 2002, Fig. 1).
223. Postclypeus: 0, not reaching dorsum of head (Dmitriev 2002, Fig. 2); 1, reaching dorsum.
224. Acrometope: 0, absent; 1, present (Dmitriev 2002, Fig. 1).
225. Head with acrometope: 0, not rounded; 1, rounded or secondarily flattened. Taxa with state 0 for character 224 are scored as? for this character.
226. Carina on head without acrometope: 0, absent; 1, along ecdysial line; 2, above ecdysial line.
227. Brush of short setae on anterior surface of middle tibia: 0, absent; 1, present.
228. Macrochaetae on head and thorax: 0, absent; 1, present.
229. Abdominal chaetotaxy: 0, unspecialized (setae scattered); 1, specialized (setae arranged in groups and/or restricted to certain parts of each segment).

Phylogenetic Analysis

Phylogenetic analysis was conducted using TNT ver. 1.5 (Goloboff and Catalano 2016) under the maximum parsimony (MP) criterion using the New Technology Search (with default algorithms: ratchet, sectorial searches, drifting, and fusing) and equal weighting with 1,000 random addition replicates (random seed = 10). All characters were treated as unordered (nonadditive) in all analyses. Branch support was assessed by jackknifing in TNT with deletion probability of 36% for 10,000 replicates and the traditional search option. Bremer support (decay index) was calculated using TNT by performing a separate heuristic search and retaining trees up to 15 steps longer than the original most parsimonious trees. Character changes were mapped on one of the original most parsimonious trees using default options in WinClada ver. 1.00.08 (Nixon 2002). A separate analysis was performed under the maximum likelihood (ML) criterion using IQtree v.2.1.3 (Nguyen et al. 2015, Minh et al. 2020) with the MK model for unordered categorical data, empirical character state frequencies, Gamma distribution for rate heterogeneity across sites, and the correction for ascertainment bias applied. This model was selected by comparing BIC scores using ModelFinder (Kalyaanamoorthy et al. 2017). Branch support was assessed using the Shimodaira-Hasegawa approximate likelihood ratio test (SH-aLRT, Guindon et al. 2010) and 1,000 ultrafast boostrap replicates (Hoang et al. 2018). To further examine the stability of phylogenetic relationships across analytical methods, a Bayesian analysis

was conducted using MrBayes 3.2 (Ronquist et al. 2012) with flat priors and Markov Chain Monte Carlo search for 10 million generations with the first 25% discarded as burn-in and trees sampled every 1,000 generations. Convergence and parameter mixing were considered sufficient when effective sample size was greater than 200 and standard deviation of split frequencies was less than 0.05.

The dataset used for all analyses is available from the Illinois Data Bank at https://doi.org/10.13012/B2IDB-6965685_V1.

Nomenclature

This paper and the nomenclatural act(s) it contains have been registered in Zoobank (www.zoobank.org), the official register of the International Commission on Zoological Nomenclature. The LSID (Life Science Identifier) number of the publication is: urn:lsid:zoobank.org:pub:B6A8A1F3-919D-4AB0-A811-BC203FFA4B62.

Results

Maximum parsimony analysis of 229 discrete morphological characters yielded 7 equally parsimonious trees of length 2,824, consistency index 0.111, and retention index 0.583. A majority-rule consensus of these trees is shown in Fig. 1. One of the 7 MP trees with character changes along each branch mapped is shown in Supp Fig. S1 (online only). Differences among most parsimonious trees were limited to rearrangements within Deltocephalinae and at one node within Ledrinae and, therefore, did not affect the inferred relationships among subfamilies.

The inferred morphology-based phylogeny based on MP analysis recovered as monophyletic all currently recognized subfamilies for which more than one representative was included, with the following exceptions: 1) Aphrodinae (including Aphrodini, Euacanthellini, Portanini, and Xestocephalini) is monophyletic, excluding *Paulianiana*, the sole included representative of Sagmatiini, which was placed as sister to the remaining Membracoidea excluding Myerslopiidae; 2) of the two included representatives of Neobalinae, *Calliscarta* is sister to Neocoelidiinae + Deltocephalinae and *Chibala* is sister to Aphrodinae; 3) within Evacanthinae, Nirvanini is sister to Tungurahualini (Mileewinae) while Evacanthini + Pagaroniini is sister to Burmotettiginae; 4) within Mileewinae, Mileewini, and Tinteromini are paraphyletic with respect to Typhlocybinae and Makilingiini and Tungurahualini are paraphyletic with respect to Evacanthinae (in part); 5) *Neopsis* (Neopsini), previously included in its own subfamily (Linnavuori 1978) or as a tribe of Macropsinae (Oman et al. 1990) but recently transferred to Tartessinae (Takiya and Dietrich 2017), is derived within Eurymelinae (sensu lato). Aphrodinae (except *Paulianiana*), Bathysmatophorinae, Cicadellinae, Coelidiinae, Deltocephalinae, Eurymelinae (including *Neopsis*), Iassinae, Ledrinae, Megophthalminae, Neocoelidiinae, Signoretiinae, Tartessinae (excluding *Neopsis*), Typhlocybinae and Ulopinae are all monophyletic in the MP results.

ML analysis yielded a phylogenetic estimate (log likelihood –11812.8; Supp Fig. S2 [online only]) similar overall to the MP results. Both results include an early-diverging clade comprising treehoppers (Aetalionidae, Melizoderidae, and Membracidae) and the monophyletic cicadellid subfamilies Megophthalminae and Ulopinae. Both results also support the monophyly of the following additional cicadellid subfamilies: Bathysmatophorinae, Eurymelinae (including *Neopsis*), Iassinae, Neocoelidiinae, Signoretiinae, Typhlocybinae, and Tartessinae (excluding *Neopsis*). Areas of incongruence are limited to branches with low support (jackknife or bootstrap <70%) in one or both analyses. Notable differences between the MP and ML results include, in the latter, paraphyly of Ledrinae with respect to Hylicinae, paraphyly of Cicadellinae with respect to Signoretiinae, and nonmonophyly of Deltocephalinae with the earliest diverging lineage from the MP tree (LH178 + *Ikelebeloha*) sister to a clade comprising *Macroceratogonia* + Neocoelidiinae. The consensus tree yielded by Bayesian analysis (Supp Fig. S3 [online only]) has many branches, including the fossil taxa, placed in a large polytomy. Nevertheless, the groupings consistently recovered by this analysis are congruent with those recovered in the ML analysis.

Areas of instability in our analyses of morphological characters alone (Fig. 1, Supp Figs. S2 and S3 [online only]) are mostly confined to deep internal branches with low support pertaining to certain relationships among cicadellid subfamilies. This was also the case in recent phylogenomic analyses (Dietrich et al. 2017, Skinner et al. 2019).

Placements of the three new fossil taxa were also somewhat inconsistent among analyses. The three new genera described below, consistently form a monophyletic group but in the MP analysis they are sister to Evacanthini + Pagaroniini within a larger clade that also includes Bathysmatophorinae, while in the ML result they are sister to Bathysmatophorinae alone. The peculiar Eocene genus *Eomegophthalmus*, tentatively placed in Megophthalminae (Dietrich and Gonçalves 2014), is sister to modern Megophthalminae in the MP results but sister to Eurymelinae (in part) in the ML results. Other included fossils are placed consistently by both analyses. The extinct Cretaceous genus *Priscacutius* is sister to the two included modern representatives of Signoretiinae in both analyses, supporting its prior placement in this subfamily (Dietrich and Thomas 2018). *Qilia*, a recently described Cretaceous ledrine placed in the extinct tribe Paracarsonini (Chen et al. 2019a) is sister to the included modern Ledrinae in both ML and MP trees.

Descriptions of Taxa

Hemiptera
Membracoidea Rafinesque, 1815
Cicadellidae Latreille, 1825
Burmotettiginae Dietrich and Zhang, new subfamily

Type genus: *Burmotettix* Dietrich and Zhang, gen. nov.

Description. Head produced; eye relatively large, mesal margin entire; crown depressed and well delimited; ocelli on crown near margin anterad of eyes; crown-face transition rounded. Face in profile forming approximately 45° angle with crown; frontoclypeus relatively narrow and moderately to strongly convex, shagreen; lateral frontal sutures poorly delimited, apparently extended dorsad from antennal ledges to crown margin but not onto crown; antennal ledge carinate, only slightly produced over antennal pit; antenna usually longer than head width; area between frontoclypeus and eye relatively broad; anteclypeus moderately convex, tapered from base to apex, or parallel-sided, extended to lower margin of face; lorum flat, poorly delimited; gena narrow, strongly emarginate below eye, exposing large, flaplike proepisternum; rostrum narrow, tapered, extended beyond front trochanters. Pronotum as wide as or wider than head; lateral margins long, divergent posterad, sharply carinate, lateral carina even with posterior corner of eye; surface minutely

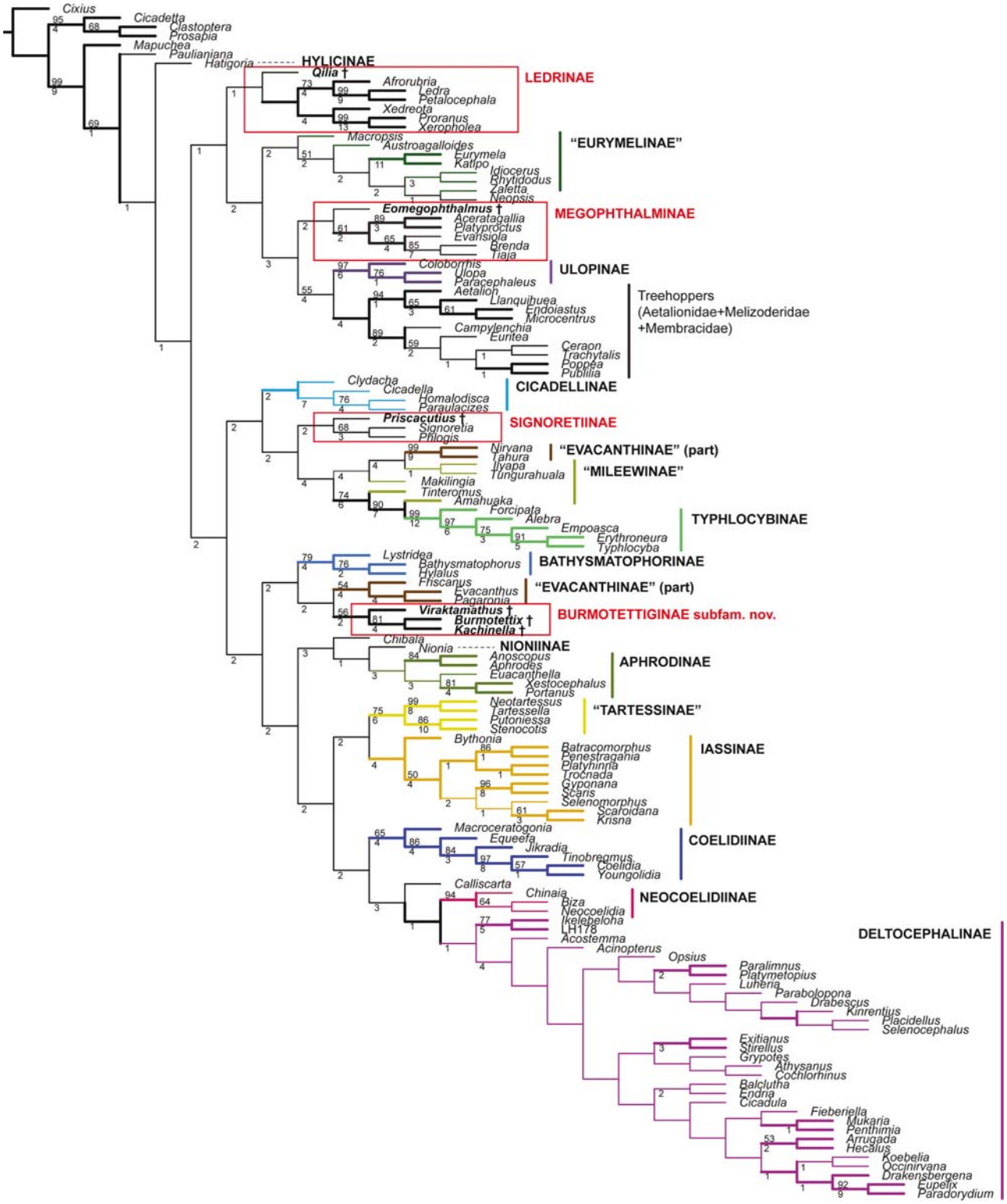

Fig. 1. Majority rule consensus of seven equally parsimonious trees for Membracoidea based on 229 unordered, equally weighted morphological characters (L = 2,824, CI = 0.11). Jackknife proportions (50% or higher) are shown above branches and Bremer support is shown below branches. Branches without Bremer support were not recovered in all equally parsimonious trees. Subfamilies including fossil taxa are enclosed in rectangles with fossils indicated by †. Character changes are shown in Supp Fig. S1 [online only].

punctate, with indistinct transverse rugae, anterior margin weakly produced, posterior margin concave or straight and exposing posterior part of mesonotum. Scutellar suture arcuate. Wings fully developed, rounded apically, forewing apices not overlapping at rest, appendix very narrow, inner apical cell tapered, extended to or near apical margin; vein M with two branches, R with three branches, crossveins s (i-r) and r-m1 present; m-cu2 usually present; inner apical cell tapered, with outer basal angle basad of inner angle, not

extended to wing apex. Hind wing submarginal vein complete, not extended onto jugum, RA2 extended to apex, RP and MA separate apically, connected by short r-m crossvein, MP and CuA separate throughout length, connected by oblique m-cu crossvein. Front leg with chaetotaxy well differentiated; femur with pair of dorsoapical macrosetae; AM1 large and situated near midheight of anterior surface, additional AM setae present or absent; IC row with several setae, AV row with few macrosetae on basal half, PV1 large; tibia with AD and PD rows with approximately equal numbers of widely spaced macrosetae. Middle tibia with AD and AV rows well developed with several macrosetae. Hind femur with apical macrosetae 2 + 2 + 1 or 2 + 1, often with additional setae more basad; tibia with four well developed rows of macrosetae; AD with smaller setae between successive macrosetae; tarsi long and slender, tarsomere I with dorsoapical pair of macrosetae and one or two ventral longitudinal rows of stout setae, pecten with platellae and tapered macrosetae; tarsomeres I and II each with two long apical macrosetae on mesal surface of apex, usually much longer than adjacent setae of pecten. Female pregenital sternite large, more than twice as long as preceding sternite, covering base of ovipositor. Male subgenital plates fused medially, genital capsule with conspicuous macrosetae.

Diagnosis. Burmotettiginae may be distinguished from other groups of leafhoppers by the following unique combination of traits: ocelli on crown near anterior margin in front of eyes; frontoclypeus strongly convex but relatively narrow compared to distance between frontoclypeus and eye; gena strongly emarginate below eye, exposing proepisternum; hind tarsomeres I and II each with pair of long preapical macrosetae on medial surface. The chaetotaxy of the hind tarsus is unique among known leafhoppers and unites the three genera here included in the subfamily, all described as new below.

Comparative notes. Burmotettiginae exhibit morphological traits present in several modern leafhopper subfamilies that have not been documented in leafhoppers described from the lower Cretaceous, suggesting that such traits first evolved sometime between 118 and 90 million years ago. In particular, the leg chaetotaxy of the new subfamily is considerably more differentiated, with all of the setal groups recognized by Rakitov (1998) clearly distinguishable. On the front femur, AM1 is enlarged, IC is represented by a single row of relatively thin setae, AV has stout setae in the basal half, and PV is also well developed in two of the three included genera. The front tibia has rows AD and PD represented by a few large, evenly spaced macrosetae. *Kachinella* and *Viraktamathus* also have an accessory longitudinal row of setae in the basal half of the front tibia between rows AD and AV, as in modern Bathysmatophorinae, Coelidiinae, Neobalinae, Tartessinae, and some Evacanthinae and Neocoelidiinae. The hind femur has the dorsoapical macrosetae reduced in number and enlarged and the rows of the hind tibia also approximate the levels of differentiation present in many modern subfamilies. The hind tibia also has the compressed shape present in modern groups such as Deltocephalinae.

As reflected by the phylogenetic placement of Burmotettiginae in a clade comprising Bathysmatophorinae and Evacanthinae, the structure of the head of Burmotettiginae is somewhat similar to that of the latter two subfamilies in having the gena strongly emarginate and the crown well delimited with the ocelli posterad of the anterior margin and well separated from the eyes (Fig. 9d and i). The above mentioned traits are also shared by some members of the modern tribe Thymbrini (subfamily Tartessinae) (Evans 1966: Fig. 19 F1, P2). However, the face of Burmotettiginae differs from Thymbrini having the distance between the frontoclypeus and eye narrower and the anteclypeus not extended beyond the lower margin of the maxillary plates (cf. Figs. 4b, f and 7a, f to Evans 1966: Fig 19 J2). The truncate apex of the anteclypeus, even with the lower genal margins in Burmotettiginae is shared with members of several modern cicadellid subfamilies, including Deltocephalinae and Iassinae (Fig. 9c and e).

Due to the presence of unique features not present in modern leafhoppers (e.g., the enlarged distal setae of hind tarsomeres I and II) Burmotettiginae does not appear to be directly ancestral to any modern cicadellid group. Presumably it represents an extinct, early diverging lineage of the crown group of Cicadellidae that includes most of the modern subfamilies with well-differentiated leg chaetotaxy (e.g., Aphrodinae, Cicadellinae, Coelidiinae, Deltocephalinae, Tartessinae, Typhlocybinae). Among modern leafhoppers, some members of Iassinae (Gyponini), Deltocephalinae, Coelidiinae, and Tartessinae have a single enlarged medioapical seta on hind tarsomeres I and II but none are as large, proportionately, as those found in Burmotettiginae and other medial setae are either small or absent in these modern groups. The tarsi of Burmotettiginae are also unusually elongate and slender compared to those of most modern leafhoppers.

***Burmotettix* Dietrich and Zhang, gen. nov.**

Type species. *Burmotettix depressa* Dietrich and Zhang, sp. nov., here designated.

Description. Small, slender, somewhat elongate leafhoppers. Head with crown depressed, shagreen, angulately produced medially, ocelli near anterior margin anterad of eyes, closer to adjacent eye than to midline, coronal suture represented by median longitudinal groove; face with frontoclypeus relatively narrow, moderately convex, broadened slightly dorsad toward antennal pit, shagreen, without punctures; antennal ledge arcuate but neither carinate nor produced over antennal base; antenna with flagellum longer than twice width of head; clypeal suture poorly delimited; lorum broad, flat, narrowly separated from lateral genal margin; anteclypeus convex, narrow, tapered from base to apex; rostrum extended well posterad of front trochanters. Forewing with three anteapical cells, outer one open or closed (crossvein s present or absent); crossvein r-m1 oblique, joining R at or very near RP branch; RA1 arising well distad of RP and extended obliquely distad to costa; brachial cell parallel-sided for most of length; CuA extended obliquely distad to point just distad of claval apex; inner apical cell slightly tapered and not extended to wing apex; claval veins distinct, parallel to each other; texture of membrane uniform throughout, appendix weakly developed. Hind wing submarginal vein complete but not extended onto jugum, narrowly separated from apical margin; RA joining RP along apical margin; RP separate from MA throughout length, joined by short r-m crossvein; MP separating from MA slightly beyond wing midlength; m-cu crossvein oblique, slightly longer than r-m crossvein but much shorter than segment of MP basad of crossvein; Pcu and A1 fused in basal half, widely divergent distally; A2 well developed and free. Front trochanter with three long setae on anterior surface. Front femur row AM with only enlarged AM1 present, IC row with several widely spaced thin setae; AV1 not well differentiated from IC setae; PV setae absent. Front tibia rows AD, PD, and AV each with four widely spaced macrosetae, respectively; without accessory setal row between AD and AV. Hind femur macrosetal formula 2 + 2 + 1 with posterior seta of penultimate pair relatively short and close to anterior seta. Hind tibia row PD with macrosetae longer

and more numerous than AD setae; AD with small setae between macrosetae; AV setae usually restricted to distal half; PV with numerous setae, alternating short and long near apex. Hind tarsomere I with dorsoapical pair of macrosetae and plantar row of short stout setae, pecten with 1 tapered lateral seta and 3–4 platellae; tarsomeres I and II each with pair of tapered medioapical setae much longer than adjacent platellae. Female sternite VII much longer than sternite VI, emarginate posteriorly; ovipositor extended slightly beyond apex of pygofer. Male genital capsule with rows of macrosetae on pygofer or subgenital plate; subgenital plates fused along midline except at apex.

Etymology. The genus name combines *Burmo-*, referring to the former name of the country of origin (Burma), with Greek: τέττιξ, τέττῑγος, tettix—cicada. Gender: masculine.

Notes. *Burmotettix* differs from the other two genera of Burmotettiginae (*Kachinella* and *Viraktamathus*, described below) in its smaller size and less developed chaetotaxy of the front and hind legs. Particularly notable is the 2 + 2 + 1 macrosetal formula of the hind femur, which is characteristic of modern cicadellid subfamilies Deltocephalinae, Coelidiinae, Neocoelidiinae, and some members of Aphrodinae and Iassinae. The structure of the male subgenital plates, which are fused medially except at the apex, is similar to the condition occurring in Neocoelidiinae. The row of lateral setae on the male pygofer of the type species is unknown among modern leafhoppers except in the nymphs of some groups (e.g., Tartessinae).

Burmotettix depressus **Dietrich and Zhang, sp. nov**
(Figs. 2A–D and 4A, B, J, K)

Description. Length including forewing 4.0 mm; head width 0.9 mm; pronotum width 0.9 mm; forewing length 3.2 mm; front femur length 0.8 mm; front tibia length 0.7 mm; hind femur length 1.0 mm; hind tibia length 1.8 mm. Overall coloration light brown without distinct pattern. Head in dorsal view with anterior margin of crown forming slightly acute angle, as long as width between eyes at base. Pronotum 1.38× longer than crown. Scutellum and exposed part of mesonotum together slightly longer than pronotum. Hind tibia rows PD, AD, AV, and PV with 13, 11, 9, and ~22 macrosetae, respectively. PD setae longer than AD setae; PV with 4 long setae in distal half separated by one shorter seta half as long. Male pygofer with lateral longitudinal row of 6 macrosetae; fused subgenital plates slender and relatively elongate, gradually tapered from base to near apex, extended slightly beyond pygofer apex in ventral view, apices slightly expanded and divergent along midline, each with pair of short setae apically and one seta near midlength.

Etymology. The species name is derived from the Latin participle *depressus* (depressed) and refers to the relatively depressed appearance of the holotype, possibly an artifact of preservation.

HOLOTYPE male. NWAFU specimen # HF00001, originating from Hukawng Valley, Kachin, Myanmar (NWAFU).

Condition. The specimen is well preserved, embedded in a clear medium yellow piece of amber with most features visible in dorsal view except parts of the right legs are obscured by a fracture, and some distortion of the face and legs has occurred due to shrinkage. The piece also contains a small hymenopteran (Mymaridae?).

Burmotettix brunnescens **Dietrich and Zhang, sp. nov.**
(Figs. 2E–G and 4C)

Description. Length including forewing 4.0 mm; head width 0.9 mm; pronotum width 1.0 mm; forewing length 3.0 mm; front femur length 0.7 mm; front tibia length 0.8 mm; hind femur length 1.3 mm; hind tibia length 2.1 mm; ovipositor length 1.2 mm; exposed part of ovipositor length 1.0 mm. Overall coloration dark brown without distinct pattern. Head in dorsal view with anterior margin of crown forming obtuse angle, slightly shorter than width between eyes at base. Pronotum 1.32× longer than crown. Scutellum and exposed part of mesonotum together slightly shorter than pronotum. Front tibia rows PD, AD, and AV with 4, 4, and 2 macrosetae, respectively, middle two setae of AD half as long as basal and distal setae. Hind tibia rows PD, AD, AV, and PV with 13, 7, ~10, and ~21 macrosetae, respectively. Female sternite VII twice as long as sternite VI; posterior margin with rounded medial notch and paired sublateral lobes.

Etymology. The species name, a non declinable Latin adjective *brunnescens* (brownish), refers to the uniformly dark brown coloration.

HOLOTYPE female: Specimen # INHSP-10329, originating from Hukawng Valley, Kachin, Myanmar (INHS).

Condition. The specimen is well preserved in a piece of clear medium yellow amber with most features visible in dorsal and ventral aspects but parts of the wings distorted and obscured dorsally by air bubbles and a small fracture partly obscuring the face. The piece also includes three globular springtails (Symphypleona).

Burmotettix limpidus **Dietrich and Zhang, sp. nov.**
(Figs. 3A–D and 4D, H, I)

Description. Length including forewing 3.8 mm; head width 0.7 mm; pronotum width 0.8; forewing length 3.3 mm; front tibia length 0.7 mm; hind tibia length 1.8 mm. Head in dorsal view with anterior margin of crown rounded with obtuse apical angle. Pronotum 1.4× longer than crown. Scutellum and exposed part of mesonotum together subequal to pronotum in length. Hind tibia rows PD, AD, AV, and PV with 20, 10, ~14, and 20 macrosetae, respectively.

Etymology. The species name is derived from the Latin adjective *limpidus* (transparent) and refers to the transparency of parts of the exoskeleton of the type specimen.

HOLOTYPE female (? apex of abdomen mostly obscured by air bubble): NWAFU specimen # HF00002, originating from Hukawng Valley, Kachin, Myanmar (NWAFU).

Condition. The specimen is well preserved, embedded in a pale yellow piece of amber with most features visible in dorsal and ventral views. The left wings are spread and perpendicular to the body with the venation clearly visible. The exoskeleton is partially translucent with some internal features visible.

Burmotettix ruber **Dietrich and Zhang, sp. nov.**
(Figs. 3E–G and 4E, F, L–N)

Description. Length including forewing 3.9 mm; head width 0.9 mm; pronotum width 0.9 mm; forewing length 3.2 mm; front femur length 0.8 mm; front tibia length 0.7 mm; hind femur length 1.0 mm; hind tibia length 1.8 mm; ovipositor length

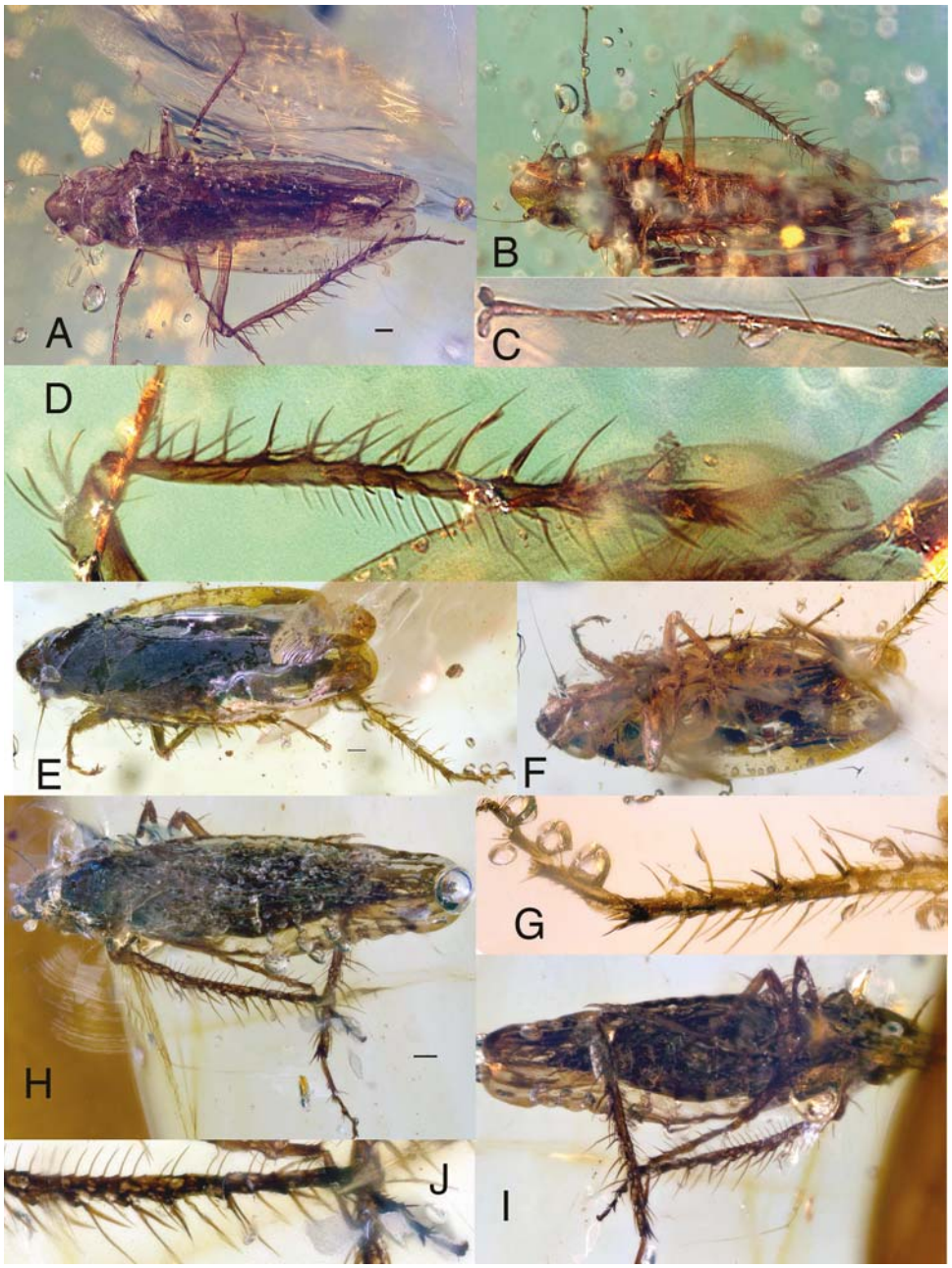

Fig. 2. Species of *Burmotettix* gen. nov., holotypes. (A–D), *B. depressus* sp. nov.: (A), dorsal habitus; (B), ventral habitus; (C), left front tibia and tarsus, dorsal view; (D), left hind leg, ventral (anterior) view. (E–G), *B. brunnescens* sp. nov.: (E), dorsolateral habitus; (F), ventral habitus; (G), distal part of right hind tibia and tarsus, ventral (anterior) view. (H–J), *B. rugosus* sp. nov.: (H), dorsal habitus; (I), ventral habitus; (J), distal part of left hind tibia and tarsus, dorsal (posterior view). Scale bars 0.2 mm.

1.2 mm; exposed part of ovipositor length 0.8 mm. Dorsum brown marked with dark reddish pigment; pronotum uniformly red, forewing with irregular red flecks. Head in dorsal view with anterior margin of crown forming slightly acute angle, as long as width between eyes at base. Pronotum 1.30× longer than crown. Scutellum and exposed part of mesonotum slightly subequal in length to pronotum. Front tibia rows PD, AD, and AV with 3, 2 and 3 macrosetae, respectively. Hind tibia rows PD, AD, AV, and PV with ~15, 9, 8, and 21 macrosetae, respectively. Female sternite VII posterior margin obtusely emarginate. Other structural features as described for genus.

Etymology. The species name is a Latin adjective *ruber* (red) refers to the red pigmentation visible on the pronotum and forewing of the holotype.

HOLOTYPE female: NWAFU specimen # HF00003, originating from Hukawng Valley, Kachin, Myanmar (NWAFU).

Condition. The specimen is well preserved, embedded in a yellow-orange piece of amber, with most features visible in dorsal and ventral view. The head and tarsomeres I and II appear to be somewhat distorted by shrinkage. The wing venation is obscured by appression to the sides of the thorax and abdomen and wrinkling.

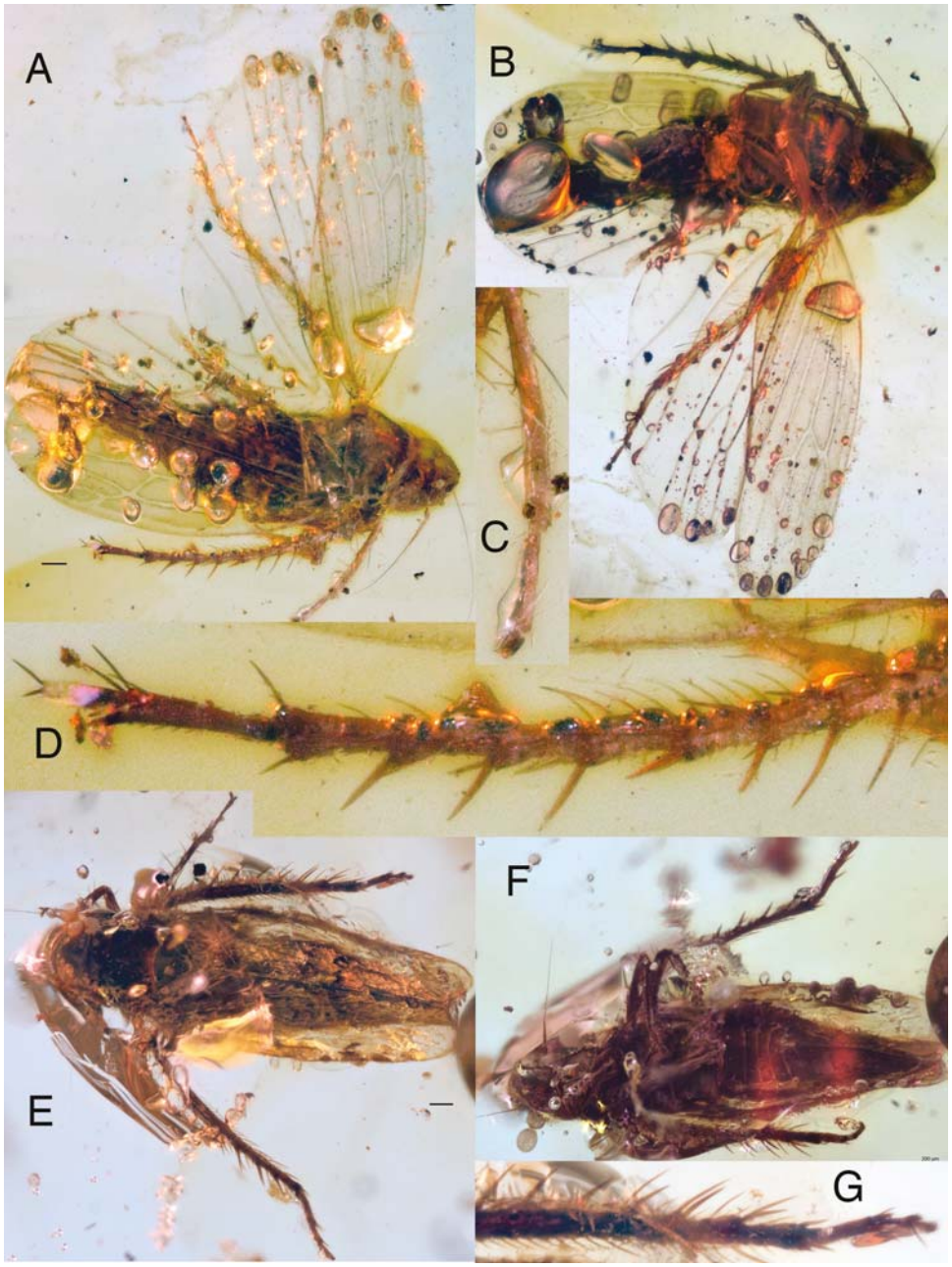

Fig. 3. Species of *Burmotettix* gen. nov., holotypes. (A–D), *B. limpidus* sp. nov.: (A), dorsolateral habitus; (B), ventrolateral habitus; (C), right front tibia and tarsus, posterodorsal view; (D), right hind tibia and tarsus (part), posterodorsal view. (E–G), *B. ruber* sp. nov.: (E), dorsal habitus; (F), ventral habitus; (G), distal part of right hind tibia and tarsus, posterodorsal view. Scale bars 0.2 mm.

***Burmotettix rugosus* Dietrich and Zhang, sp. nov.**
(Figs. 2H–J and 4G)

Description. Length including forewing 3.9 mm; head width 0.8 mm; pronotum width 0.9; forewing length 3.2 mm; front femur length 0.7 mm; front tibia length 0.6 mm; hind femur length 1.3 mm; hind tibia length 1.8 mm. Head in dorsal view with anterior margin of crown acutely produced and angulate, slightly longer than basal width between eyes. Pronotum subequal to crown in length and slightly shorter than exposed part of mesonotum and scutellum. Hind tibia rows PD, AD, AV, and PV with 17, 10, 10, and 24 macrosetae, respectively; PD setae alternating short and long. Subgenital plates short and relatively broad, partly concealed by pregenital sternite, rounded apically, each with 2 elongate, stout setae apically extended posterad.

Etymology. The species name, which is a Latin adjective *rugosus* (wrinkled), refers to the rugose texture of the dorsum of the holotype, probably an artifact of preservation.

HOLOTYPE male: NWAFU specimen # HF00004 originating from Hukawng Valley, Kachin, Myanmar (NWAFU).

Condition. The specimen is moderately well preserved, embedded in a pale yellow piece of amber with most features visible in dorsal and ventral views. The exoskeleton is opaque and the wing venation

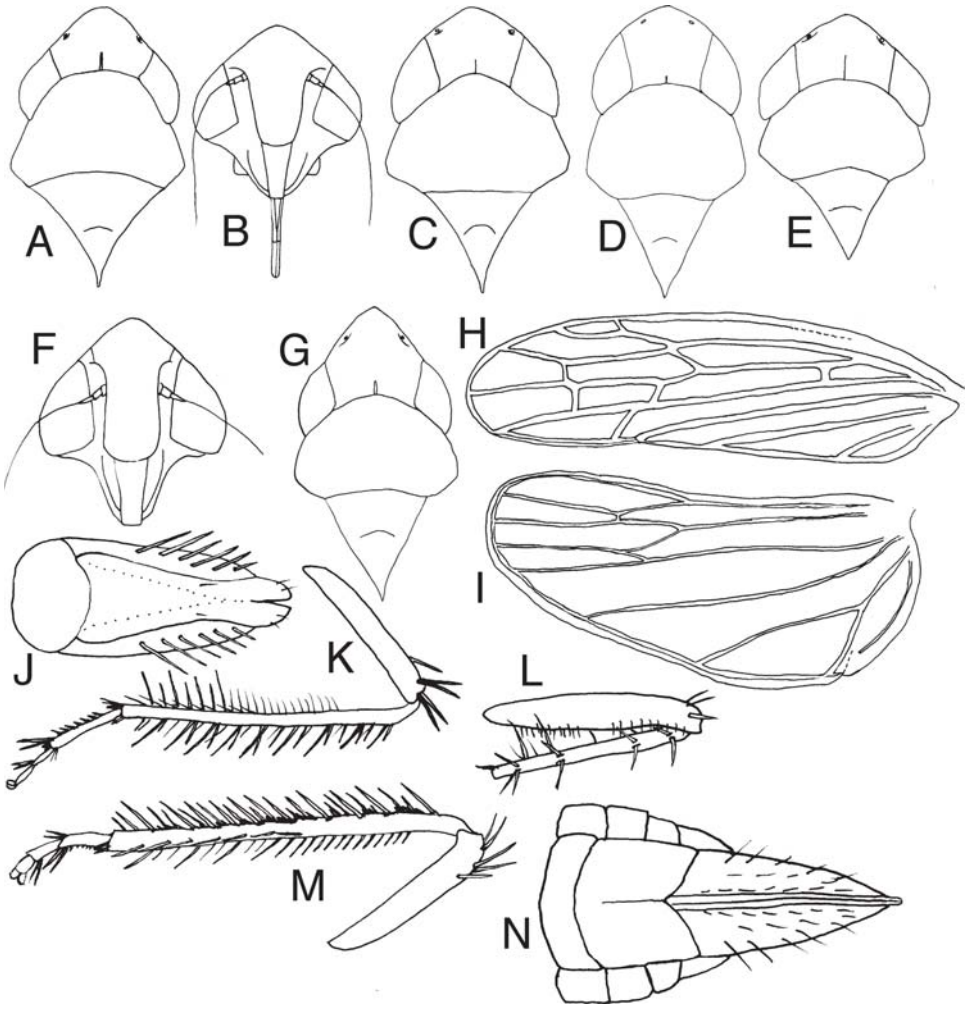

Fig. 4. Species of *Burmotettix* gen. nov. (A), *B. depressus* sp. nov., head, pronotum, mesonotum, and scutellum, dorsal view; (B), same, face, anteroventral view. (C), *B. brunnescens* sp. nov., head, pronotum, mesonotum, and scutellum, dorsal view. (D), *B. limpidus* sp. nov., same. (E), *B. ruber* sp. nov., same; (F), *B. ruber* sp. nov., face, anteroventral view. (G), *B. rugosus* sp. nov., head, pronotum, mesonotum, and scutellum. (H, I), *B. limpidus* sp. nov., fore- and hind-wing. (J), *B. depressus* sp. nov., male genital capsule, ventral view; (K), hind leg, anteroventral view. (L–N), *B. ruber* sp. nov.: (L), front femur and tibia, anterior view; (M), hind leg, anteroventral view; (N), apex of female abdomen, ventral view.

is mostly obscured due to appression against the sides of the body. The texture of the dorsal integument is highly rugulose but this appears to be an artifact of preservation. There is substantial apparent shrinkage and flattening of the face and legs.

***Kachinella* Dietrich and Zhang, gen. nov.**

Type species: *Kachinella bicolor* Dietrich and Zhang, sp. nov.

Description. Medium sized, slender, elongate. Head with crown depressed, shagreen, angulately produced medially, ocelli near anterior margin anterad of eyes, closer to adjacent eye than to midline, coronal suture represented by indistinct median longitudinal carina; face with frontoclypeus relatively narrow, broadened slightly dorsad toward antennal pit, shagreen and sparsely punctate; antennal ledge arcuate and carinate but not strongly produced over antennal base; antenna with flagellum longer than twice width of head; clypeal suture poorly delimited; lorum broad, flat, narrowly separated from lateral genal margin; anteclypeus slightly broadened from base to apex, with median longitudinal fold (possibly a preservation artifact) and pair of short setae preapically, apex truncate, and even with lower margin of maxillary plate; rostrum extended slightly beyond front trochanters. Pronotum with lateral margin approximately as long as eye. Forewing venation poorly delimited, texture of membrane smooth, uniform throughout, appendix weakly developed; inner apical cell tapered from base to apex, extended to apical margin; apical cells 2 and 3 widened distally, apical cell 2 shorter than 3; RA1 arising distad of RP, two r-m crossveins present, crossvein m-cu2 apparently absent. Hind wing fully developed with submarginal vein narrowly separated from apical margin. Front trochanter with three long anterior setae on anterior surface. Front femur with four AM setae in row basad of enlarged AM1, IC row with ~12 widely spaced thin setae; AV with 5–6 long stout widely spaced setae in basal half, AV1 not well differentiated from IC setae; PV1 large and one additional PV seta near midlength and one at base. Front tibia rows AD and PD with five and four widely spaced macrosetae, respectively, AD row with smaller setae between macrosetae, ventral rows with several widely spaced setae, accessory setal row present between AD and AV in basal half. Front tarsus more than half as long as tibia; tarsomere I with two long apical ventral setae and few shorter preapical setae. Middle femur slightly shorter and taller than front femur; AD and AV each with several macrosetae. Middle tibia with dorsal rows 5 + 5. Hind femur macrosetal formula 2 + 1

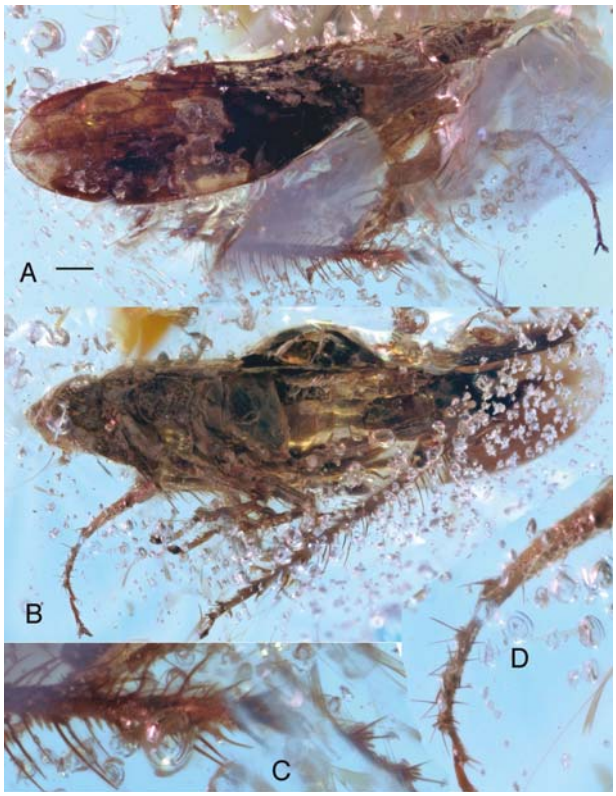

Fig. 5. *Kachinella bicolor* sp. nov., female holotype: (A), lateral habitus; (B), ventrolateral habitus; (C), distal part of left hind tibia and tarsus, posteroventral view; (D), right front femur, tibia, and tarsus, anteroventral view. Scale bar 0.5 mm.

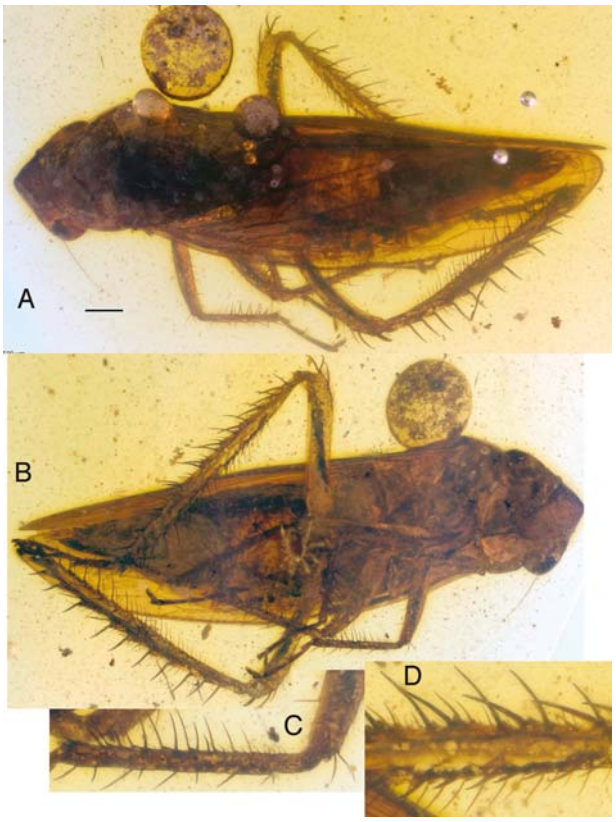

Fig. 6. *Viraktamathus burmensis* sp. nov., female holotype: (A), dorsolateral habitus; (B), ventrolateral habitus; (C), left front femur and tibia, anteroventral view; (D), right hind tibia (basal half), anteroventral view. Scale bar 0.5 mm.

with several smaller setae more basad in dorsal row. Hind tibia rows PD, AD, AV, and PV with approximately 15, 10, 9, and 23 macrosetae, respectively; AD with small cucullate setae between macrosetae; PD with alternating long and short macrosetae, both longer than AD macrosetae; AV row restricted to distal half of tibia. Hind tarsomere I with dorsoapical pair of macrosetae and plantar row of short stout setae, pecten with 1 tapered (medial) seta and 3 platellae; tarsomeres I and II each with pair of medioapical setae much longer than adjacent platellae. Female sternite VII without conspicuous setae, twice as long as sternite VI, posterior margin truncate; ovipositor extended well beyond apex of pygofer. Male unknown.

Etymology. The new genus is named for the state (Kachin) in which the holotype was collected. Gender: feminine.

Notes. The presence of an accessory longitudinal row of stout setae between rows AD and AV on the front femur is shared with modern subfamilies Coelidiinae, Neobalinae, Tartessinae, and Neocoelidiinae. A preapical pair of setae on the anteclypeus also occurs in some Coelidiinae and Neocoelidiinae but both of these modern subfamilies lack crossvein r-m1 in the forewing. *Kachinella* also differs from all four of these modern subfamilies in the structure of the head (e.g., emarginate gena exposing proepisternum), forewing (e.g., reduced appendix), and other aspects of the leg chaetotaxy of the front femur (e.g., presence of preapical AM and PV setae), and hind femur (2 + 1 apical macrosetae and additional dorsal setae more basad) and tibia (AV restricted to distal half).

Kachinella bicolor **Dietrich and Zhang, sp. nov.**
(Figs. 5 and 7A–E)

Description. Length including forewing 7.9 mm; head width 1.1 mm; pronotum width 1.4 mm; forewing length 6.3 mm; front femur length 1.2 mm; front tibia length 1.1; hind femur length 2.7 mm; hind tibia length 3.2 mm; ovipositor length 1.8 mm; exposed part of ovipositor 0.9 mm. Head, pronotum, mesonotum, and scutellum pale yellow; pronotum with three small brown spots posteriorly, one medial and one on each lateral corner. Forewing pale yellow in basal fourth, dark brown distally except for irregular medial pale area (possibly a preservation artifact). Pronotum 1.57× longer than crown. Scutellum and exposed part of mesonotum 1.33× longer than crown. Other structural features as described for genus.

Etymology. The species name name is a nondeclinable Latin adjective *bicolor* (two-colored); it refers to the bicolored pattern of the dorsum.

HOLOTYPE female. NWAFU specimen # HF00005, originating from Hukawng Valley, Kachin, Myanmar (NWAFU).

Condition. The specimen is well preserved, embedded in a yellow-orange piece of amber. The head and distal tarsomeres appear to be somewhat distorted by shrinkage. Fractures and numerous air bubbles in the amber obscure the view of the anterior part of the head on the right side, the pronotum in left lateral view, and parts of the legs and abdomen in ventral view. The hind wing is also not visible.

Viraktamathus **Dietrich and Zhang, gen. nov.**

Type species: *Viraktamathus burmensis* Dietrich and Zhang, sp. nov.

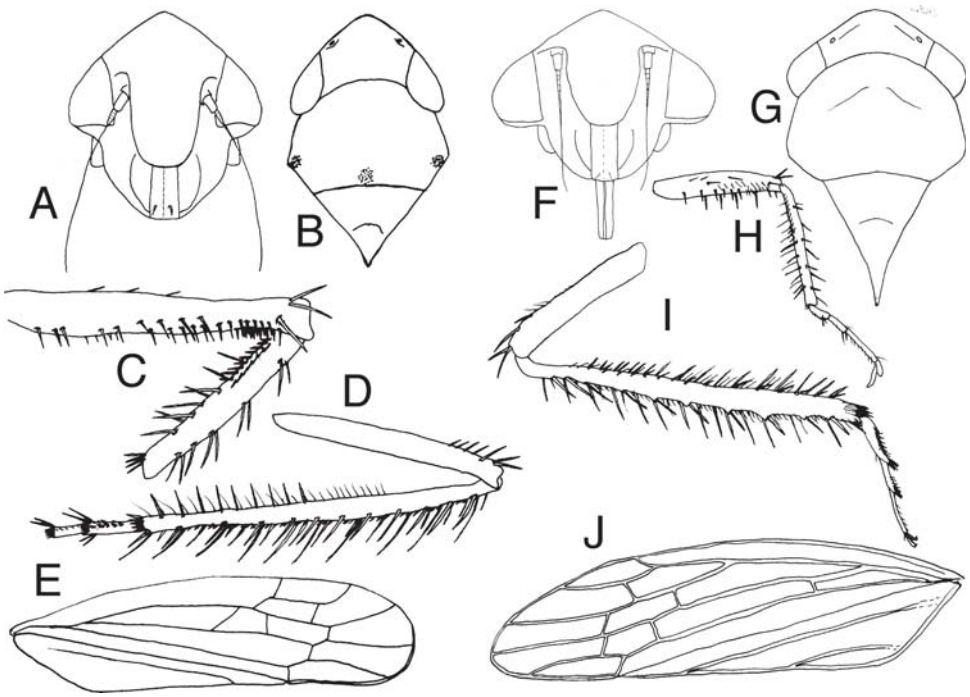

Fig. 7. (A–E), *Kachinella bicolor* sp. nov: (A), head, anteroventral view; (B), head, pronotum, mesonotum, and scutellum, dorsal view; (C), left front femur and tibia, anterior view; (D), left hind femur, tibia and first two tarsomeres; (E), forewing. (F–I), *Viraktamathus burmensis* sp. nov: (F), head, anteroventral view; (G), head, pronotum, mesonotum, and scutellum, dorsal view; (H), left front femur, tibia, and tarsus, anterior view; (I), right hind femur, tibia, and tarsus, anterior view; (J), forewing.

Description. Crown short, anterior margin angulate in dorsal view, surface longitudinally rugose posteromedially; ocelli on crown near anterior margin in oblique grooves, slightly closer to eyes than to midline, bounded posteromedially by oblique carina parallel to anterior crown margin. Antennal ledge situated just below crown margin, obliquely carinate, encroaching onto frontoclypeus, not concealing antennal base in anterior view; antenna length less than width of head; frontoclypeus strongly swollen, separated from adjacent eye by half frontoclypeal width, finely rugose and sparsely punctate with muscle scars visible dorsally; gena acutely emarginate below eye, exposing flaplike proepisternum; anteclypeus convex, slender, approximately parallel sided, with pair of small setae preapically; lorum flat, well separated from margin of face; rostrum slender, slightly surpassing front trochanter, two distal segments subequal in length. Pronotum enlarged; lateral margins as long as eye, sharply carinate, carina even with posterior corner of eye, divergent posterad; surface conspicuously punctate and irregularly transversely striate, posterior margin slightly concave, not extended to scutellar suture. Exposed part of mesonotum shagreen, weakly concave; scutellar suture poorly delimited, arcuate; scutellum acuminate and depressed. Forewing extended well beyond apex of abdomen at rest, texture smooth except sparsely punctate along costal margin in basal two thirds and at base of clavus, apex obliquely rounded, not overlapping other forewing at rest, crossveins s (i-r), r-m1, and m-cu2 present (with three closed subapical cells); apical cells 2–4 slightly broadened distally, appendix narrow, extended to apex. Hind wing fully developed, venation apparently complete, submarginal vein well separated from apical margin, R2 + 3 not extended to apex, outer apical cell unusually large, twice as wide as adjacent apical cell.

Front femur row AV with 5 long setae widely spaced in basal half and 3 short preapical setae; AD1 and PD1 well developed; IC row with 8 well spaced setae, few not aligned with others; AM1 at midheight of femur, 3 additional enlarged AM setae present near midlength of femur; PV1 present and row PV with 5 more evenly spaced preapical setae. Front tibia row AD with 4 and PD with 5 evenly spaced macrosetae; with accessory row of ~6 short setae in basal half between AD and AV; AV with 5 large distinct setae distally and 12 small basal setae; PV with 7 macrosetae. Front tarsus more than half as long as tibia. Middle leg with femur more robust than front femur, AD row with numerous macrosetae; AV row with 6 macrosetae, AM row well differentiated at midheight. Middle tibial rows PD, AD, AV, and PV with 6, 6, 10, and 15 (6 large) setae, respectively. Hind femur with 2 apical macrosetae, 1–2 large preapical AD setae and ~8 smaller, widely spaced setae more basad. Hind tibia rows PD, AD, AV, and PV with 13, 1–11, 14–15, and 29–33 macrosetae, respectively; AD with setal bases prominent, spinelike distally and with 3–9 small setae between successive macrosetae also on prominent bases; PD with 2–4 smaller setae between long macrosetae; PV with 6 preapical setae each separated by 2 smaller setae; tarsomere I only slightly longer than II and III, with two well developed plantar rows of cucullate setae each with ~7 setae, PV setae as long as width of tarsomere, AV setae shorter and stouter, pecten with 4 platellae, outer and inner tapered setae and pair of long inner apical setae, dorsoapical pair poorly differentiated.

Female with abdominal sternite VII twice as long as sternite VI, with pair of submedial longitudinal rows of stout setae, posterior margin concave. Ovipositor extended well beyond apex of pygofer.

Male unknown.

Etymology. The genus is named for Prof. Chandra A. Viraktamath, University of Agricultural Science, Bengaluru (Bangalore), India, in recognition of his many outstanding contributions to knowledge of Cicadellidae. Gender: masculine.

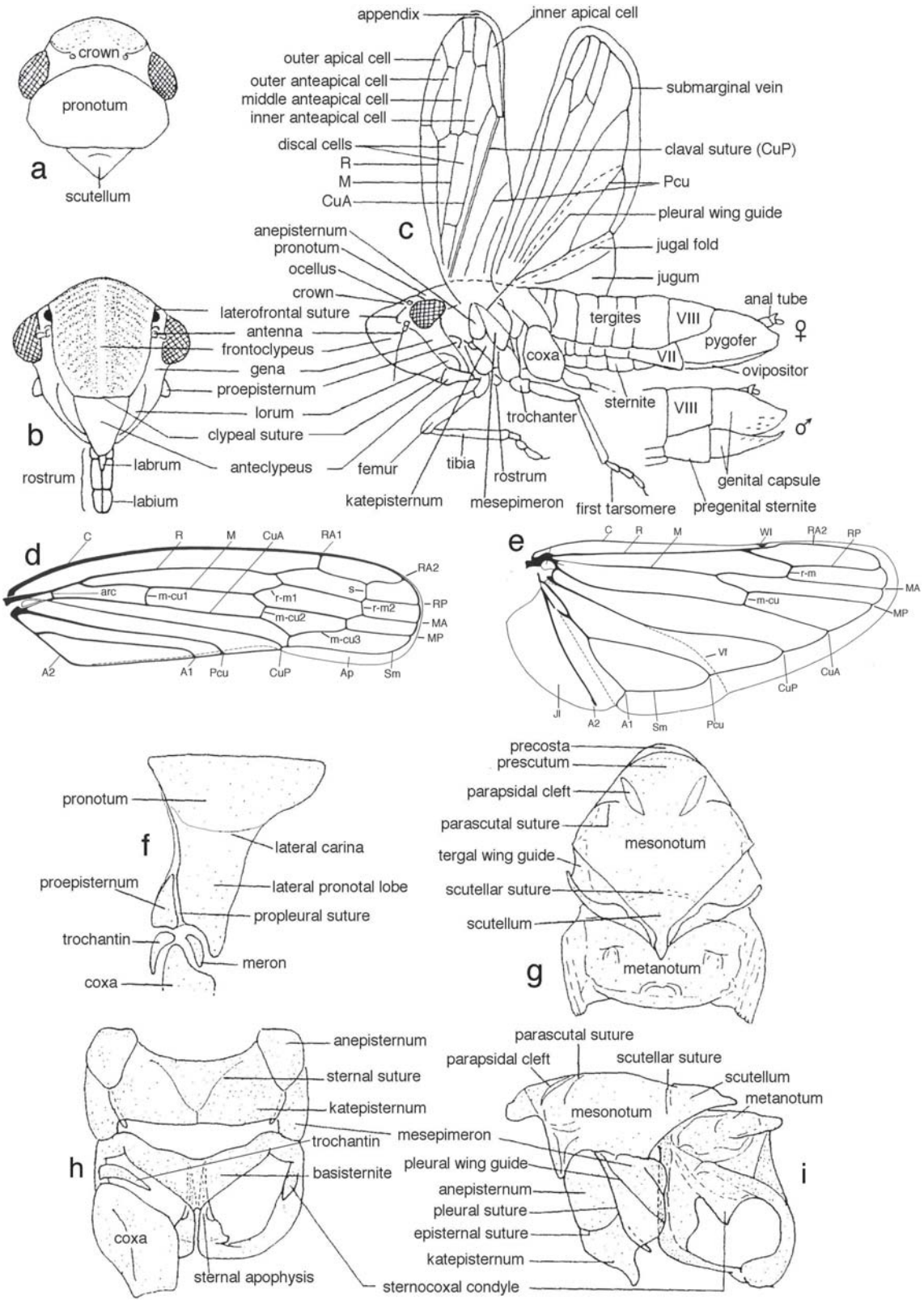

Fig. 8. General terminology for external morphological structures of Cicadellidae. (a), head and part of thorax, dorsal view; (b), head, anteroventral view; (c), whole body with wings spread, lateral view, with male and female terminalia shown; (d), forewing; (e), hind wing; (f), prothorax, lateral view; (g), meso- and meta-thorax, dorsal view; (h), same, ventral view; (i), same, lateral view.

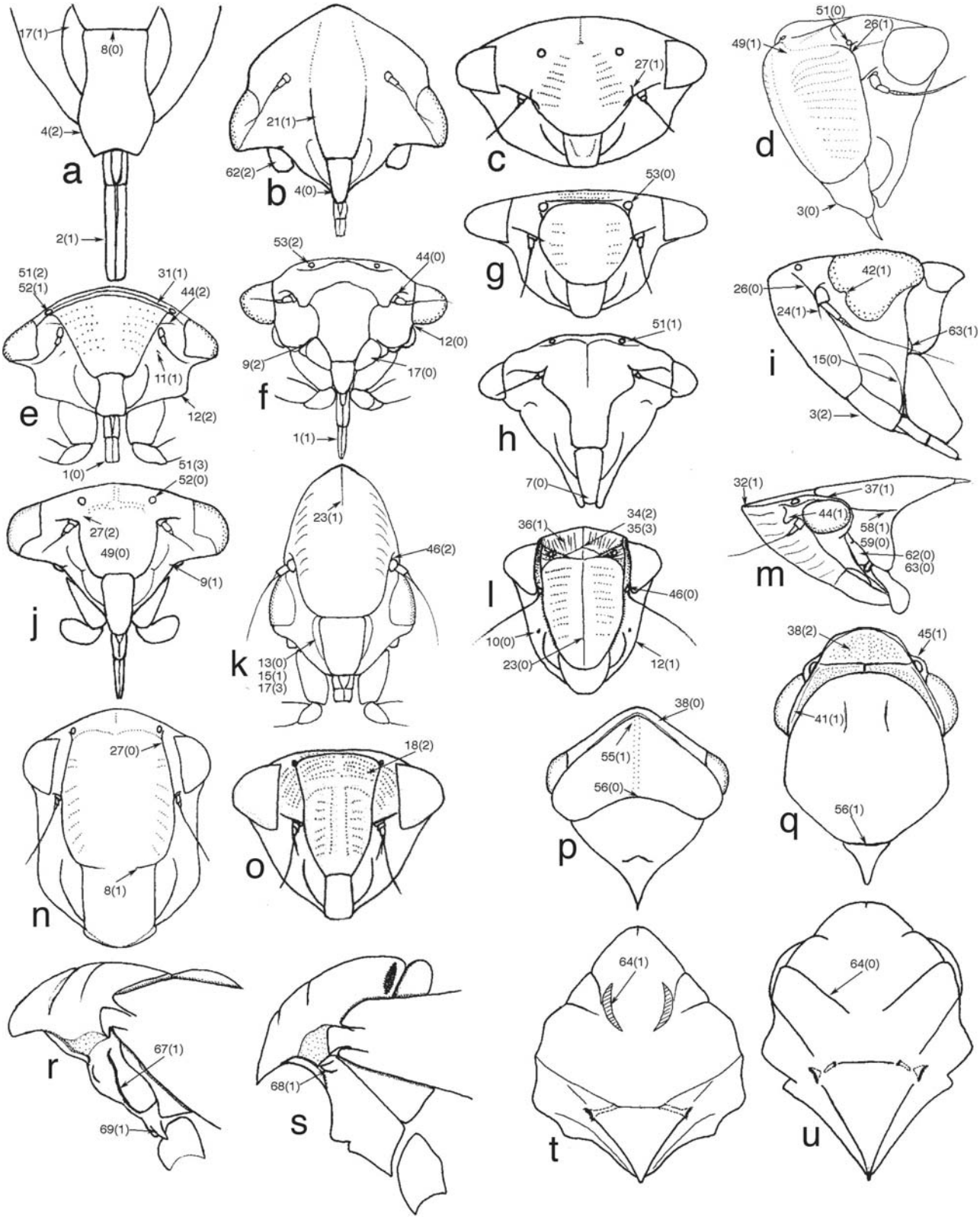

Fig. 9. Structures of the head and thorax with labels numbered according to the character (and state) listed in the Methods Section. (a), *Tinobregmus viridescens* (Coelidiinae), lower part of face, anterior view; (b), *Petalocephala* sp. (Ledrini), anteroventral view of head; (c), *Gargaropsis* sp. (Iassini), anterior view of head; (d), *Evacanthus* sp. (Evacanthini), anterolateral view of head; (e), *Adama* sp. (Selenocephalini), anteroventral view of head and front leg bases; (f), *Mesargus* sp. (Ulopini), anterior view of head; (g), *Bythonia* sp. (Bythoniini), anterior view of head; (h), *Kyphocotis* sp. (Stenocotini), anteroventral view of head; (i), *Portanus* sp. (Portanini), lateral view of head and prothorax (part); (j), *Platyproctus* sp. (Adelungiini), anteroventral view of head and front leg bases; (k), *Nirvana* sp. (Nirvanini), same; (l), *Onukia burmanica* (Evacanthini), anterior view of head; (m), *Signoretia* sp. (Signoretiini), lateral view of head and prothorax (part); (n), *Balala* sp. (Hylicini), anterior view of head; (o), *Neotartessus* sp. (Tartessini), anterior view of head; (p), *Macropsis* sp. (Macropsini), dorsal view of head, pronotum, and mesonotum; (q), *Signoretia* sp., same; (r), *Coloborrhis corticina* (Ulopinae), lateral view of mesothorax (part); (s), *Telamona* sp. (Membracidae), same; (t), *Coloborrhis corticina*, dorsal view of thorax (pronotum removed); (u), *Aetalion reticulatum*, same.

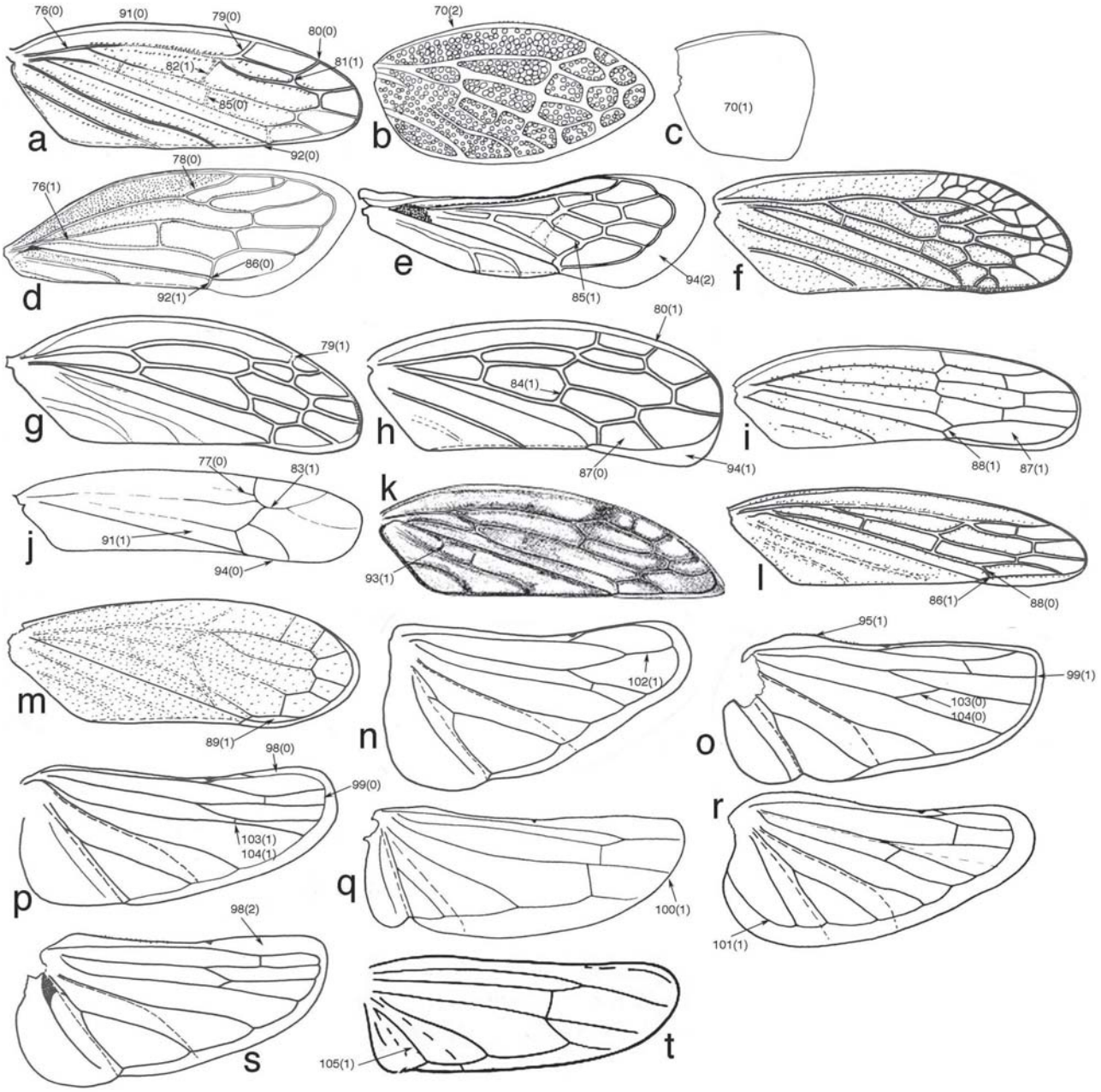

Fig. 10. Wings labeled with characters and states as in Fig. 9. (a–m), forewings: (a), *Aphrodes* sp.; (b), *Ulopa* sp.; (c), *Drakensbergena* sp.; (d), *Membracis* sp.; (e), *Hylica* sp.; (f), *Ledra* sp.; (g), *Agallia* sp.; (h), *Deltocephalus* sp.; (i), *Cicadella* sp.; (j), *Typhlocyba* sp.; (k), *Acinopterus* sp.; (l), *Gypona* sp.; (m), *Iassus* sp. (n–t), hind wings: (n), *Iassus* sp.; (o), *Mileewa* sp.; (p), *Acostemma* sp.; (q), *Typhlocyba* sp.; (r), *Tartessus* sp., (s), *Cicadella* sp.; (t), *Erythroneura* sp.

Notes. *Viraktamathus* is similar to other Burmotettiginae in several respects, including the structure of the head, forewing venation, and leg chaetotaxy, but the lateroapical setae of hind tarsomeres I and II are not elongated as in other members of the subfamily. *Viraktamathus* seems most similar to modern representatives of the subfamily Tartessinae, particularly members of the Australian endemic tribe Thymbrini, in having the head with a well-developed crown and preapical ocelli, the anterior margin of the pronotum strongly produced, and the hind leg with several prominent setae between successive macrosetae on tibial row AD. The presence of spinelike setal bases on this row and the relatively wide distance between the frontoclypeus lateral margin and the eye indicate possible affinity with Ledrinae. The presence of a distinct accessory setal row between rows AD and AV on the front tibia is shared with some modern leafhoppers and also with *Kachinella* (above). *Viraktamathus* differs from *Kachinella* in having the medioapical setae of the first and second hind tarsomeres no longer than the adjacent setae of the apical pecten. Nevertheless, the head morphology and wing venation suggest that this genus is a close relative of other Burmotettiginae.

Viraktamathus burmensis **Dietrich and Zhang, sp. nov.**
(Figs. 6 and 7F–J)

Description. Body length including forewings at rest 7.9 mm; head width 1.6 mm; pronotum width 1.8 mm; forewing length 6.0 mm;

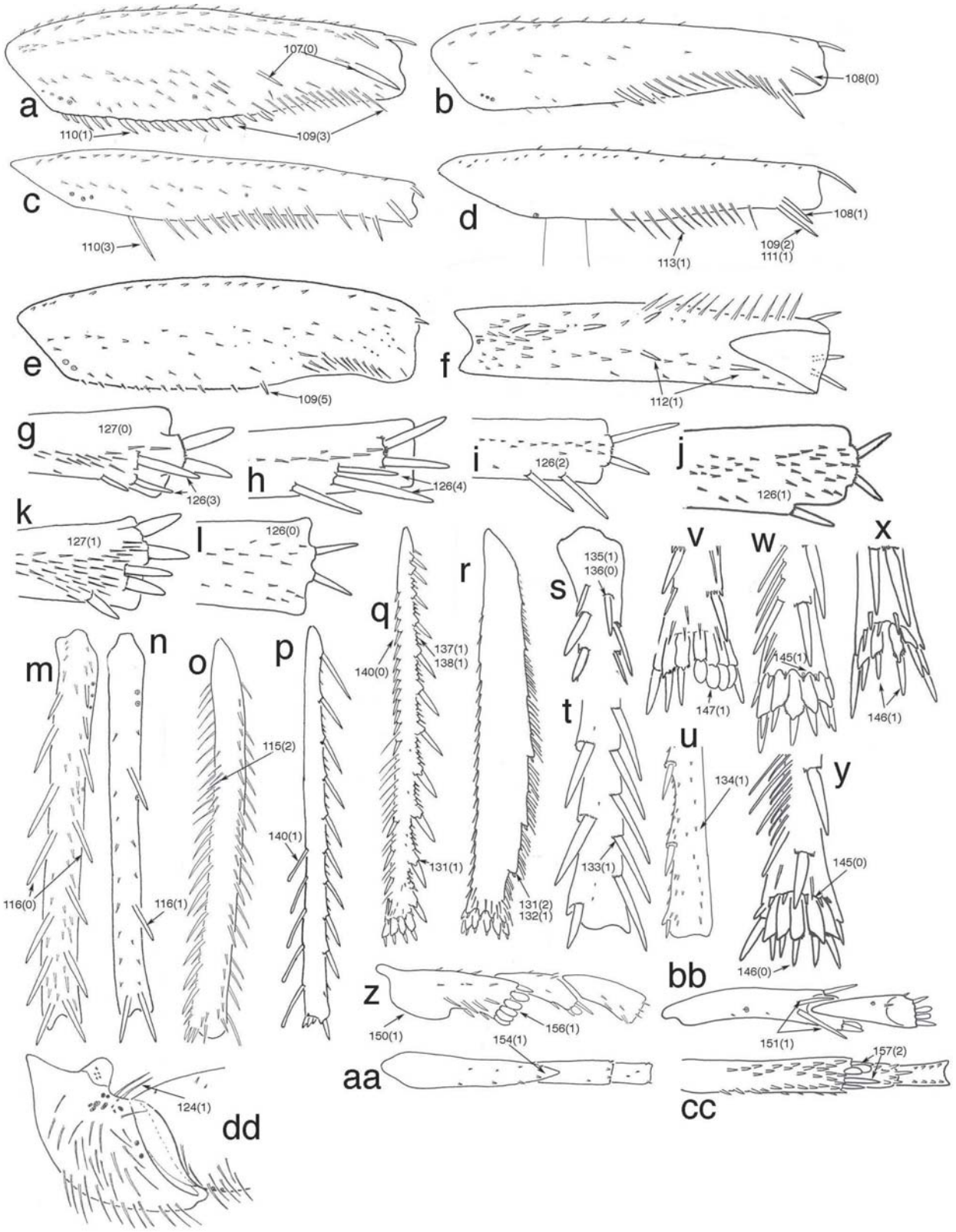

Fig. 11. Legs labeled with characters and states as in Fig. 9. (a–e), front femur, anterior view: (a), *Selenocephalus* sp.; (b), *Cicadella* sp.; (c), *Nirvana* sp.; (d), *Mileewa* sp.; (e), *Evansiola* sp. (f), *Gypona* sp., front femur, ventral view; (g–l), hind femur apex, dorsal view: (g), *Coelidia* sp.; (h), *Deltocephalus* sp.; (i), *Tinteromus* sp.; (j), *Agallia* sp.; (k), *Penthima* sp.; (l), *Idiocerus* sp. (m, n), front tibia, dorsal view: *Selenocephalus* sp.; (n), *Deltocephalus* sp.; (o–r), hind tibia, anterior view: (o), *Coelidia* sp.; (p), *Typhlocyba* sp.; (q), *Tartessus* sp.; (r), *Ledra* sp.; (s), *Coelidia* sp., hind tibia base, dorsal view; (t, u), hind tibia apex, dorsal view: (t), *Gypona* sp.; (u), *Signoretia* sp.; (v–y), hind tibia apex, ventral view: (v), *Eupelix* sp.; (w), *Gypona* sp.; (x), *Deltocephalus* sp.; (y), *Coelidia* sp.; (z), *Eupelix* sp., hind tarsus, lateral view (part). (aa), *Typhlocyba* sp.; (bb), *Deltocephalus* sp., hind tarsus, dorsal view (part); (cc), *Agallia* sp. hind tarsus, ventral view (part); (dd) *Rhytidodus* sp., hind trochanter and base of femur.

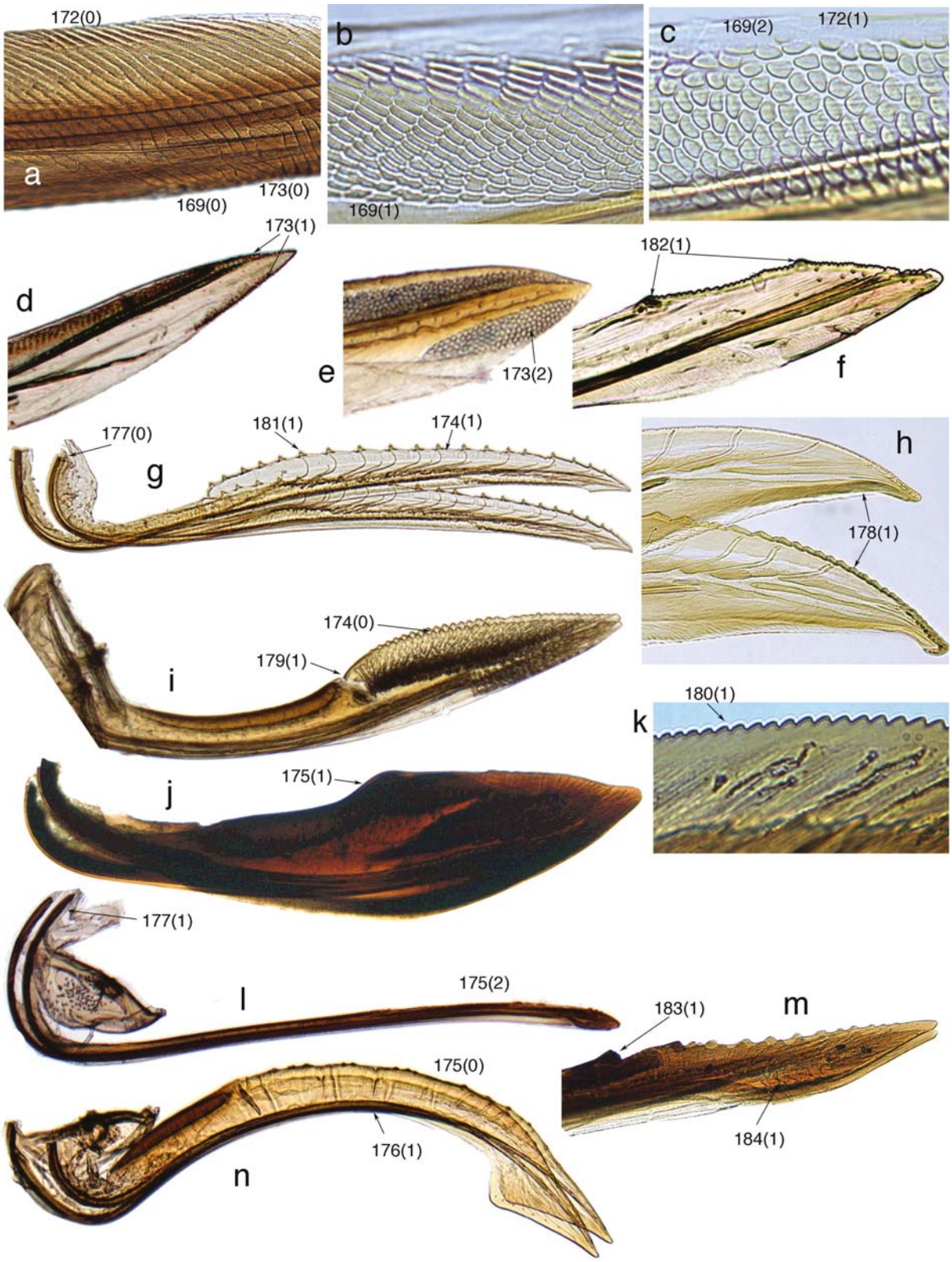

Fig. 12. Ovipositors labeled with characters and states as in Fig. 9. (a–c), first valvula dorsal sculpture: (a), *Ledra* sp.; (b), *Evansiola insularis*; (c), *Drakensbergena* sp.; (d, e), first valvula apex: (d), *Batracomorphus* sp.; (e), *Paradorydium* sp.; (f–n), second valvulae: (f), *Batracomorphus* sp., apex; (g), *Graphocephala* sp.; (h), *Dikraneura* sp., apices; (i), *Evacanthus* sp.; (j), *Scaris* sp.; (k), *Evansiola insularis*, enlargement of dorsal margin; (l), *Macropsis* sp.; (m, n), *Xestocephalus* sp.; (k–l), second valvulae apex: (k), *Batracomorphus* sp.; (l, m), *Tinobregmus* sp. apex.

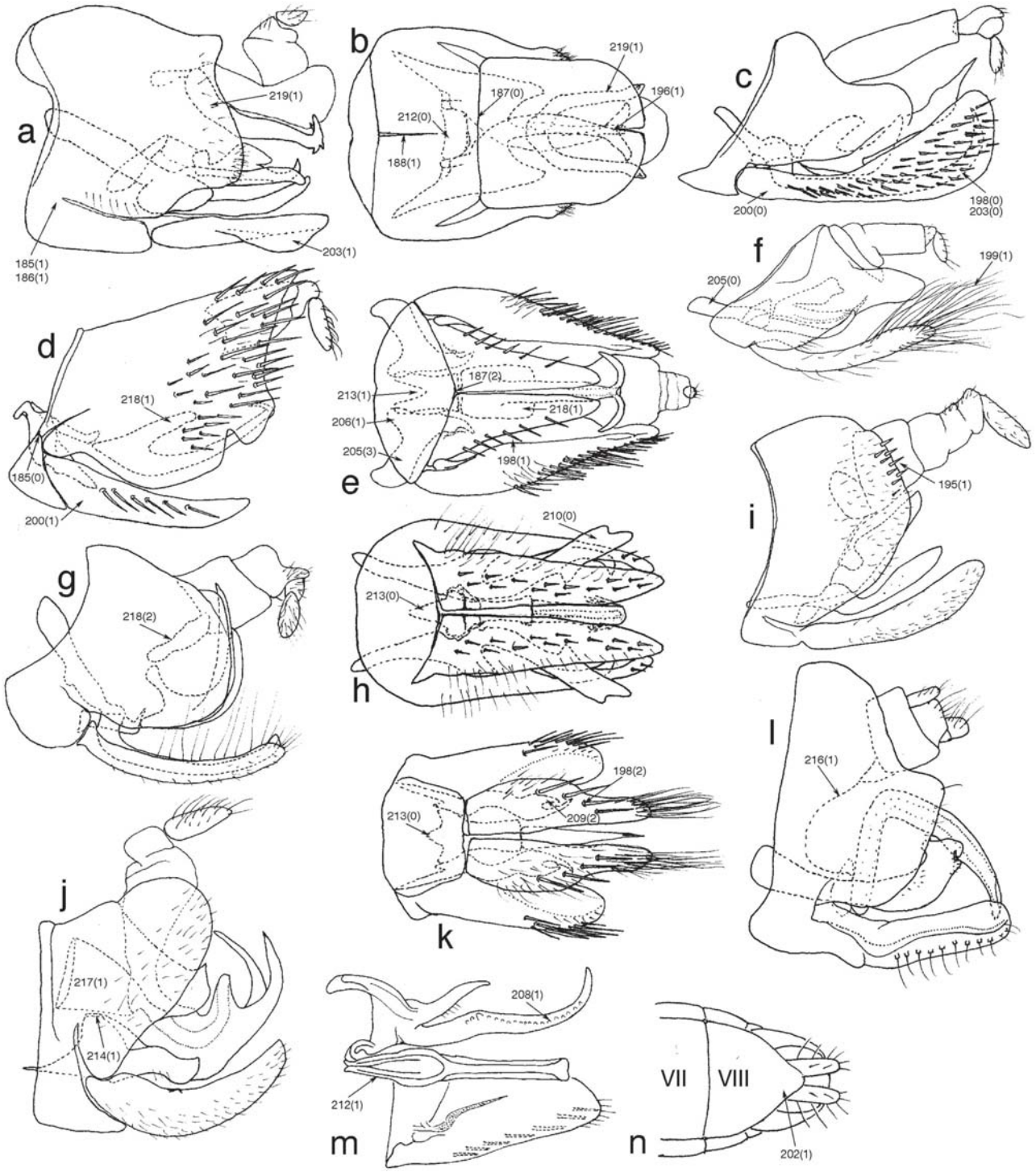

Fig. 13. Male genital capsule with characters and states labeled as in Fig. 9. (a, b), *Tiaja* sp., lateral and ventral views; (c), *Calliscarta* sp., lateral view; (d–e), *Hecalus* sp., lateral and ventral view; (f), *Idiocerus* sp., lateral view; (g), *Macropsis* sp., lateral view; (h), *Lystridea* sp., ventral view; (i), *Xerophloea* sp., lateral view; (j), *Paraulacizes* sp., lateral view; (k), *Portanus* sp., ventral view; (l), *Myerslopia* sp., lateral view. (m), Paralimnini, style, connective, and subgnenital plate, dorsal view. (n), Iassini, male terminalia with most of genital capsule concealed ventrally by enlarged sternite VIII.

front femur length 1.3 mm; front tibia length 1.3 mm; hind femur length 2.3 mm; hind tibia length 3.7 mm; ovipositor length 2.3 mm (1.6 mm exposed beyond sternite VII). Structural features as described for genus.

Etymology. The species epithet refers to the historical name of Myanmar, Burma.

HOLOTYPE female : Cretaceous Myanmar amber, NWAFU specimen # HF00006 originating from Hukawng Valley, Kachin, Myanmar (NWAFU).

Condition. The specimen is well preserved in a clear piece of medium yellow amber with most structures visible in dorsal and ventral aspect and apparently only minor shrinkage and distortion due to preservation.

Discussion

Phylogenetic analyses of morphological characters using both maximum parsimony (MP) and maximum likelihood criteria (ML) yielded well-resolved trees that are consistent in many respects (cf. Fig. 1, Supp Fig. S2 [online only]), including recovering most currently recognized cicadellid subfamilies as monophyletic. These analyses also consistently agree with prior morphology-based analyses (Hamilton 1983, Dietrich 1999) indicating that Cicadellidae is paraphyletic with respect to a lineage comprising the three currently recognized families of treehoppers (Aetalionidae, Melizoderidae, and Membracidae). The results based on morphological characters alone also generally agree with those of the most extensive previous molecular phylogenetic analysis of Membracoidea (Dietrich et al. 2017) including support for the monophyly of many cicadellid subfamilies as currently defined. Comparison of these recent results suggests that morphology is reliable for diagnosing monophyletic groups (e.g., subfamilies) of Membracoidea, but that some relationships among major lineages of Membracoidea are proving difficult to resolve consistently with either molecular or morphological data.

Our morphology-based MP analyses provide support for some groups that recent molecular phylogenies failed to recover. These include Aphrodinae (excluding *Paulianiana*), Coelidiinae (including *Equeefa*), Eurymelinae (including *Austroagalloides*), Iassinae (including *Bythonia*), Ledrinae, and Tartessinae (including *Neopsis* in the ML analysis). In the phylogenomic analysis of Dietrich et al. (2017), branches separating different representatives of these subfamilies were unstable and received low branch support; therefore, support for their nonmonophyly was also low. Nevertheless, in agreement with recent molecular phylogenies, our morphology-based analyses consistently indicate that Mileewinae (sensu Dietrich 2011) is paraphyletic, placing *Amahuaka* (Mileewini), and *Tinteromus* (Tinteromini) in a paraphyletic grade subtending Typhlocybinae. Evacanthinae is recovered as monophyletic in the ML analysis of morphological characters, in agreement with the molecular phylogeny of Dietrich et al. (2017), but this subfamily is paraphyletic in the MP results. Another notable difference between the MP and ML analyses of morphological characters is the placement in the latter of *Neopsis* as sister to the remaining Tartessinae but as a derived lineage of Eurymelinae in the MP analysis.

The ML and MP results are largely consistent in their placements of the included fossils. *Qilia* is consistently sister to the included modern representatives of Ledrinae and *Priscacutius* is sister to modern representatives of Signoretiinae, in agreement with their previous placements in these subfamilies (Dietrich and Thomas 2018, Chen et al. 2019a). Relationships among the three newly described genera (Burmotettiginae) are consistent across analyses but placement of this group relative to other cicadellid subfamilies is somewhat inconsistent. In the MP trees this clade is sister to Evacanthinae (in part) within a larger clade also comprising Bathysmatophorinae; in the ML tree, Burmotettiginae is sister to Bathysmatophorinae alone. *Eomegophthalmus*, a remarkable taxon from Eocene Baltic amber suggested to possibly represents the stem group from which Megophthalminae, Ulopinae, and treehoppers arose (Dietrich and Gonçalves 2014), is sister to the modern Megophthalminae in the MP trees but sister to Eurymelinae in the ML tree, highlighting its mixed morphological affinities. This instability in placement of some fossil taxa may be partly due to the large amounts of missing data in the fossils but could also reflect the overall paucity of stable morphological synapomorphies defining subfamilies and other major lineages of Membracoidea. Although the three genera of Burmotettiginae are united by the unique chaetotaxy of the hind tarsi, they otherwise appear to have mixed morphological affinities to various extant cicadellid subfamilies (see Comparative Notes under subfamily treatment above).

Unfortunately, although recent molecular phylogenetic analyses based on both transcriptomes (Skinner et al. 2019, Hu et al. 2022) and anchored hybrid data (Dietrich et al. 2017) have provided support for many currently recognized leafhopper subfamilies and generally agree with the morphology-based phylogenetic estimates presented here, these prior analyses have failed to resolve relationships among major lineages consistently, with many very short, deep internal branches receiving low support. This suggests that Membracoidea underwent an ancient rapid radiation, with most modern subfamilies appearing over a relatively short time interval during the Cretaceous (Dietrich et al. 2017).

Notes on Cretaceous-age Fossil Leafhoppers

Although the oldest known Cicadellidae are recorded from the lower Cretaceous (Shcherbakov 1986, Hamilton 1990) and molecular divergence time analyses suggest that most of the modern subfamilies of leafhoppers arose during the early to middle Cretaceous (Dietrich et al. 2017), very few Cretaceous-age leafhopper fossils are known (reviewed by Chen et al. 2021) and only three (Coelidiinae, Ledrinae, and Signoretiinae) of the 19 currently recognized modern cicadellid subfamilies are recorded from the Cretaceous (Chen et al. 2019a, 2021; Wang et al. 2019; Poinar and Brown 2020). Thus, a crucial stage in the evolution of leafhoppers is still mostly undocumented in the fossil record. The new fossil taxa described herein are important because, unlike the previously described leafhoppers from Myanmar amber, they cannot be easily accommodated in any modern cicadellid subfamily. They document a critical stage in leafhopper evolution, exhibiting many traits in common with modern leafhoppers but combinations of traits not known in the modern fauna.

Most of the leafhoppers previously reported from the Cretaceous are fragmentary and/or poorly preserved, with few diagnostic traits that would enable their relationships to modern groups to be estimated (Shcherbakov 1986, Hamilton 1992). As noted by Shcherbakov (1992), although *Paracarsonus* Hamilton and *Platyjassites* Hamilton were originally placed in Jascopidae (Hamilton 1990), the heads of these two taxa are similar in structure to those of the modern cicadellid subfamily Ledrinae. Both have the crown flattened with a distinct rim along the anterior margin, and the frontoclypeus relatively narrow compared to the distance between the frontoclypeus and the mesal margin of the compound eye. These two traits are considered to be synapomorphies shared with modern Ledrinae. Unlike modern ledrines, however, the forewings of the two fossil taxa are similar in lacking an r-m crossvein basad of the initial branch of vein M and in having vein CuA1 confluent with the posterior branch of M for a short distance but then diverging again near the wing apex. Although the leg chaetotaxy is not preserved in *Paracarsonus* and *Platyjassites*, these two forewing traits seem sufficient to justify retaining Paracarsonini Hamilton as a distinct tribe of Ledrinae. Chen et al. (2019a) noted that their fossil ledrine preserved in Myanmar amber, *Qilia regilla*, resembles *Paracarsonus* and *Platyjassites* in having the anterior margin of the crown strongly overlapping the eye anterolaterally and this possible synapomorphy helps justify their placement of *Qilia* in Paracarsonini. However, both *Qilia* and the closely related *Duyana* (Chen et al. 2021), differ from the lower Cretaceous genera previously placed in Paracarsonini in having the forewing with an r-m crossvein basad of the fork of vein M, and CuA

completely confluent with MP distally, traits more similar to those present in modern ledrines. *Qilia* (and apparently also *Duyana*) differs from modern ledrines in having the macrosetae of hind tibial row AD situated at the apex of large, spinelike bases. Modern ledrines and thymbrines also have the setal sockets of hind tibial row AD enlarged but the macrosetae originate near the base of the spine rather than at the apex.

Hamilton (1990) placed another fossil taxon, *Proerrhomus* Hamilton, in Cicadellinae, sensu lato, which he considered to include Bathysmatophorini, a group elevated to separate subfamily status by Wei et al. (2010). Although Hamilton (1990) mentioned that *Prorrhomus* is 'superficially similar to long-winged forms of the Bathysmatophorini', he also noted that the ocelli are placed farther back on the crown, as in Cicadellinae sensu stricto (Young 1968, Dietrich 2005). Based on the drawings and description provided by Hamilton (1990) the morphology of *Proerrhomus* is consistent with that of modern Cicadellinae (sensu Young 1968, Dietrich 2005) but it cannot be placed in that subfamily with certainty because the forewing apex and legs are too poorly preserved. The inflated face with frontoclypeus extended onto the crown, well developed lateral frontal sutures extended to the ocelli, placement of the ocelli near the posterior margin of the crown and coriaceous forewing are all features diagnostic for Cicadellinae. However, the hind wing venation of *Proerrhomus* sp. A (Hamilton 1990: Fig. 9, 83) is unusual in having vein RA1 unusually long (as reported in some other Cretaceous-age membracoids by Shcherbakov 1992), suggesting that this genus retains plesiomorphic hind wing venation not present in modern leafhoppers.

Two Cretaceous genera, *Ovojassus* Hamilton and *Hallex* Hamilton, placed by Hamilton (1990) in two monobasic tribes of Myerslopiidae (as Myerslopiinae) do not exhibit obvious traits that distinguish them from Cicadellidae or unequivocally unite them with modern Myerslopiidae. In his detailed morphological study of Myerslopiidae and superficially similar ground-dwelling Cicadellidae, Hamilton (1999) retained *Ovojassus* in Myerslopiidae because 'the female appears to have eight pregenital sternites' as in modern myerslopiids but the abdomen of the fossil specimen appears to be poorly preserved with segmentation difficult to discern and Hamilton's (1990) descriptions and drawings of the two included *Ovojassus* species imply that the visible enlarged and posteriorly emarginate pregenital sternite is the seventh, not the eighth. Hamilton (1999) removed Hallicini from Myerslopiidae based on the short hind basitarsomere, suggesting that it belongs to the lineage 'Ulopidae + Membracidae' but, based on the drawings provided by Hamilton (1990), only the type species has the hind basitarsomere relatively short. *Hallex gracilior* and *H. brevipes*, the only other species with the hind tarsi well preserved, have the basal tarsomere more elongate relative to the distal segments. The hind wing venation of *Ovojassus* remains unknown but, like *Proerrhomus*, *Hallex* retains a relatively long vein RA1 in the hind wing, distinguishing it from modern Membracoidea. A few fossilized forewing fragments from the lower Cretaceous previously placed in Cicadellidae, including *Acocephalites* Meunier, *Homopterulum* Handlirsch, and *Jassites* Handlirsch, were considered by Shcherbakov (1992) to belong to the extinct membracoid family Archijassidae (as Karajassidae) based on the apparently incomplete amalgamation of veins MP and CuA1. An undescribed fossil from the Purbeck Beds, Dorset, UK tentatively identified as Cicadellidae (Coram and Jepson 2012: Fig. 64) also has veins MP and CuA1 separate distally and is, therefore, more appropriately placed in Archijassidae.

Jascopus Hamilton (1971), described based on a nymph from Upper Cretaceous (Campanian, ~78 Ma) New Jersey amber, was originally placed in a separate, extinct family, Jascopidae, but later transferred to Cicadellidae by Evans (1972). Placement of this fossil remains uncertain because, unlike modern leafhoppers, it lacks longitudinal rows of setae on the hind tibia. Shcherbakov (1992, 2012) suggested that it represents an early diverging lineage of Cicadellidae with secondarily reduced hind leg chaetotaxy.

A leafhopper from the Upper Cretaceous (Maastrichtian, ~69 Ma) described based on an isolated forewing impression (Oman 1937) appears to be correctly placed in Cicadellidae and was more recently placed in Bathysmatophorinae (Szwedo 2005) but its relationship to modern leafhoppers remains uncertain because the preserved parts of the wing shape and venation are consistent with species belonging to multiple subfamilies (e.g., Iassinae and Tartessinae in addition to Bathysmatophorinae) and, therefore, not sufficient to place it precisely. Two additional nymphs in upper Cretaceous Canadian amber, identified as belonging to the cicadellid subfamily Ledrinae by K. G. A. Hamilton, were listed by Skidmore (1999) but these have not been formally described.

The fossil cicadellids from Myanmar amber described herein exhibit a unique combination of morphological traits not found in any modern leafhopper subfamily. They apparently represent a lineage distinct from previously recognized cicadellid subfamilies, supporting their placement together in a new (extinct) subfamily, Burmotettiginae. Although the three genera included in this subfamily are quite different from each other, they share a unique combination of traits, including the presence of paired, enlarged medioapical setae on the first and second hind tarsomeres, a trait not known to occur in any modern leafhopper group. Other diagnostic features of Burmotettiginae, including the narrow, emarginate gena, location of ocelli on the crown slightly posterad of the anterior margin, presence of >1 macroseta in both AM and PV rows on the front femur, and presence of an accessory setal row between AD and AV on the front tibia (in two of the three genera), occur in various modern leafhopper subfamilies but not together in the same combination.

So far, two families of Membracoidea, Cicadellidae and Archijassidae, have been recorded from the Cretaceous. The extinct family Archijassidae (subfamily Dellasharinae Shcherbakov 2012) first appeared in the Triassic and compression fossils as young as Lower Cretaceous age have been described from Eurasia, but only one archijassid, unplaced to subfamily, has been reported from Cretaceous Myanmar amber (Chen et al. 2020b). Well-preserved bizarre specimens attributed to another extinct Mesozoic superfamily of Cicadomorpha, Hylicelloidea, have also been described from Myanmar amber (Minlagerrontidae; Chen et al. 2019b, 2020a, c; Fu et al. 2020), indicating that other extinct Mesozoic lineages of Cicadomorpha survived into the late Cretaceous, coexisting with modern-looking leafhoppers belonging to the Cicadellidae.

Studies of Myanmar amber inclusions have proliferated in recent years (Ross 2019, 2020) thanks to large numbers of new specimens becoming available. So far, leafhoppers and other Membracoidea appear to be very rare but new discoveries are likely and may be expected to reveal the presence of additional modern leafhopper subfamilies, as well as extinct species that bridge morphological gaps between modern groups, during the Cretaceous. The comprehensive morphological data matrix presented here will facilitate placing newly discovered fossil Membracoidea within a phylogenetic framework.

Supplementary Data

Supplementary data are available at *Insect Systematics and Diversity* online.

Acknowledgments

We are grateful to R. A. Rakitov for helpful discussions during the development of the character list and data matrix, to S. W. Heads (INHS) for the use of his equipment to prepare and photograph the fossils included in this study, and to the editor and two anonymous referees for helpful suggestions that improved the manuscript. This work was funded in part by grants from the U. S. National Science Foundation (DEB-9978026, 0529679, 084162, 1239788 and 1639601) to CHD and DAD and from the National Natural Science Foundation of China (31420103911) to YZ that enabled the senior author to conduct research as a visiting scholar at NWAFU. DMT is a research productivity fellow from CNPq (Proc. 314557/2021-0) and a Cientista do Nosso Estado fellow from FAPERJ (Proc. E-26/202.672/2019). The opinions expressed by individuals in this report do not necessarily represent the policies of the U.S. Department of Agriculture.

Author Contributions

CD conceptualised the study, obtained funding, compiled and analysed the data and drafted the manuscript. DD contributed morphological characters and data. DT provided specimens and analysed the data. MT prepared and photographed the fossils. MW and JZ provided specimens, illustrations and data. YZ obtained funding, provided specimens and illustrations, and co-directed the research. All authors contributed to writing and editing the final version of the manuscript.

References Cited

Bisulca, C., P. C. Nascimbene, L. Elkin, and **D. A. Grimaldi. 2012.** Variation in the deterioration of fossil resins and implications for the conservation of fossils in amber. Am. Mus. Novit. 3734: 1–19.

Cao, Y., C. H. Dietrich, J. N. Zahniser, and **D. A. Dmitriev. 2022.** Dense sampling of taxa and characters improves phylogenetic resolution among deltocephaline leafhoppers (Hemiptera: Cicadellidae: Deltocephalinae). Syst. Entomol. doi: 10.1111/syen.12540.

Catanach, T. A. 2013. Biogeography and phylogenetics of grassland Auchenorrhyncha. PhD dissertation, University of Illinois at Urbana-Champaign, 133.

Chen, J., B. Wang, J. R. Jones, Y. Zheng, H. Jiang, T. Jiang, J. Zhang, and **H. Zhang. 2019a.** A representative of the modern leafhopper subfamily Ledrinae in mid-Cretaceous Burmese amber (Hemiptera, Cicadellidae). Cretaceous Res. 95: 252–259.

Chen, J., J. Szwedo, B. Wang, Y. Zheng, H. Jiang, T. Jiang, X. Wang, and **H. Zhang. 2019b.** A new bizarre cicadomorph family in mid-Cretaceous Burmese amber (Hemiptera, Clypeata). Cretaceous Res. 97: 1–15.

Chen, J., B. Wang, H. Zhang, H. Jiang, T. Jiang, Y. Zheng, and **X. Wang. 2020a.** New discovery of Minlagerrontidae in mid-Cretaceous Burmese amber (Hemiptera, Cicadomorpha, Clypeata). Cretaceous Res. 106: 104204.

Chen, J., B. Wang, Y. Zheng, H. Jiang, T. Jiang, X. Wang, and **H. Zhang. 2020b.** The youngest record of the leafhopper family Archijassidae in Kachin amber from the lowermost Upper Cretaceous of northern Myanmar (Cicadomorpha, Cicadelloidea). Cretaceous Res. 106: 104252.

Chen, J., H. Zhang, H. Jiang, Y. Li, T. Jiang, Y. Zheng, and **X. Wang. 2020c.** *Eurypterogerron kachinensis* gen. et sp. nov., a remarkable minlagerrontid (Hemiptera, Cicadomorpha) in mid-Cretaceous Burmese amber. Cretaceous Res. 110: 104418.

Chen, J., H. Jiang, T. Shang, L. Zhang, Y. Zheng, Q. Zhang, and **H. Zhang. 2021.** The second leafhopper of the subfamily Ledrinae (Hemiptera, Cicadellidae) in mid-Cretaceous Burmese amber. Cretaceous Res. 122: 104763.

Coram, R. A., and **J. E. Jepson. 2012.** Fossil insects of the Purbeck limestone group of southern England: paleoentomology from the dawn of the Cretaceous. Siri Scientific Press, Rochdale, U.K.

Dietrich, C. H. 1999. The role of grasslands in the diversification of leafhoppers (Homoptera: Cicadellidae): a phylogenetic perspective, pp. 44–48. *In* C. Warwick (ed.), Proceedings, 15th North American Prairie Conference. Natural Areas Association, Bend, Oregon, USA.

Dietrich, C. H. 2005. Keys to the families of Cicadomorpha and subfamilies and tribes of Cicadellidae (Hemiptera: Auchenorrhyncha). Fla. Entomol. 88: 502–517.

Dietrich, C. H. 2011. Tungurahualini, a new tribe of Neotropical leafhoppers, with notes on the subfamily Mileewinae (Hemiptera: Cicadellidae). ZooKeys. 124: 19–39.

Dietrich, C. H., and **L. L. Deitz. 1993.** Superfamily Membracoidea (Homoptera: Auchenorrhyncha). II. Cladistic analysis and conclusions. Syst. Entomol. 18: 297–312.

Dietrich, C. H., and **A. C. Gonçalves. 2014.** New Baltic amber leafhoppers representing the oldest Aphrodinae and Megophthalminae (Hemiptera, Cicadellidae). Eur. J. Taxon. 74: 1–13.

Dietrich, C. H., and **M. J. Thomas. 2018.** New eurymeline leafhoppers (Hemiptera, Cicadellidae, Eurymelinae) from Eocene Baltic amber with notes on other fossil Cicadellidae. ZooKeys. 726: 131–143.

Dietrich, C. H., R. A. Rakitov, J. L. Holmes, and **W. C. Black, IV. 2001.** Phylogeny of the major lineages of Membracoidea (Insecta: Hemiptera: Cicadomorpha) based on 28S rDNA sequences. Mol. Phyl. Evol. 18: 293–305.

Dietrich, C. H., D. A. Dmitriev, R. A. Rakitov, D. M. Takiya, and **J. N. Zahniser. 2005.** Phylogeny of Cicadellidae (Cicadomorpha: Membracoidea) based on combined morphological and 28S rDNA sequence data, pp. S13–14. *In* A. Purcell (ed.), Abstracts of Talks and Posters: 12th International Auchenorrhyncha Congress, Berkeley, CA, 7-12 August, 2005.

Dietrich, C. H., D. A. Dmitriev, R. A. Rakitov, D. M. Takiya, M. D. Webb, and **J. N. Zahniser. 2010.** Phylogeny of Cicadellidae (Hemiptera: Cicadomorpha: Membracoidea) based on morphological characters, pp. 48–49. *In* 13th International Auchenorrhyncha Congress Abstracts.

Dietrich, C. H., J. M. Allen, A. R. Lemmon, E. Moriarty Lemmon, D. M. Takiya, O. Evangelista, K. K. O. Walden, P. G. S. Grady, and **K. P. Johnson. 2017.** Anchored hybrid enrichment-based phylogenomics of leafhoppers and treehoppers (Hemiptera: Cicadomorpha: Membracoidea). Insect Syst. Divers. 1: 57–72.

Dmitriev, D. A. 2002. Larvae of the leafhopper subfamily Deltocephalinae (Homoptera, Cicadellidae) from European Russia and adjacent territories: 1. A key to the tribes Drabescini, Scaphytopiini, Hecalini, Limotettigini, and Opsiini. Entomol. Rev. 82: 975–1002.

Dmitriev, D. A. 2003. 3i Interactive keys and taxonomic databases. http://dmitriev.speciesfile.org/ [accessed 29 March 2022].

Emeljanov, A. F. 1987. Phylogeny of Cicadina (Homoptera) according to data on comparative morphology. Trudy Vsesoyuznogo Entomologicheskogo Obshchestva. 69: 19–109.

Engel, M. S. 2020. Myanmar: paleontologists must stop buying conflict amber. Nature. 584: 525.

Evans, J. W. 1966. The leafhoppers and froghoppers of Australia and New Zealand (Homoptera: Cicadelloidea and Cercopoidea). Mem. Aust. Mus. 12: 1–347.

Evans, J. W. 1972. Some remarks on the family Jascopidae (Homoptera, Auchenorrhyncha). Psyche. 79: 120–121.

Fu, Y., D. Azar, and **D. Huang. 2020.** A new species of the extinct family Minlagerrontidae (Insecta: Hemiptera: Cicadomorpha) from mid-Cretaceous Burmese amber. Cretaceous Res. 107: 104270.

Goloboff, P. A., and **S. A. Catalano. 2016.** TNT version 1.5, including a full implementation of phylogenetic morphometrics. Cladistics. 32: 221–238.

Guindon, S., J. F. Dufayard, V. Lefort, M. Anisimova, W. Hordijk, and **O. Gascuel. 2010.** New algorithms and methods to estimate maximum-likelihood phylogenies: assessing the performance of PhyML 3.0. Syst. Biol. 59: 307–321.

Hamilton, K. G. A. 1971. A remarkable fossil homopteran from Canadian Cretaceous amber representing a new family. Can. Entomol. 103: 943–946.

Hamilton, K. G. A. 1975. Review of the tribal classification of the leafhopper subfamily Aphrodinae (Deltocephalinae of authors) of the Holarctic region (Rhynchota: Homoptera: Cicadellidae). Can. Entomol. 107: 477–498.

Hamilton, K. G. A. 1983. Classification, morphology and phylogeny of the family Cicadellidae (Rhynchota: Homoptera), pp. 15–37. *In* W. J. Knight, N. C. Pant, T. S. Robertson, and M. R. Wilson (eds.), Proc. 1st

International Workshop on Biotaxonomy, Classification and Biology of Leafhoppers and Planthoppers of Economic Importance. Commonwealth Institute of Entomology, London.

Hamilton, K. G. A. 1990. Homoptera. *In* D. A. Grimaldi (ed.). Insects from the Santana Formation. Lower Cretaceous of Brazil. Bull. Am. Mus. Nat. Hist. 195: 82–122.

Hamilton, K. G. A. 1992. Lower Cretaceous Homoptera from the Koonwarra fossil bed in Australia, with a new superfamily and synopsis of mesozoic homoptera. Ann. Entomol. Soc. Am. 85: 423–430.

Hamilton, K. G. A. 1999. The ground-dwelling leafhoppers Sagmatiini and Myerslopiidae (Rhynchota: Homoptera: Membracoidea). Inverteb. Taxon. 13: 207–235.

Hoang, D. T., O. Chernomor, A. von Haeseler, B. Q. Minh, and **L. S. Vinh. 2018**. UFBoot2: Improving the ultrafast bootstrap approximation. Mol. Biol. Evol. 35: 518–522.

Hu, Y., C. H. Dietrich, R. K. Skinner, and **Y. Zhang. 2022**. Phylogeny of Membracoidea (Hemiptera: Auchenorrhyncha) based on transcriptome data. Syst. Entomol. doi:10.1111/syen.12563

Kalyaanamoorthy, S., B. Q. Minh, T. K. Wong, A. Von Haeseler, and **L. S. Jermiin. 2017**. ModelFinder: fast model selection for accurate phylogenetic estimates. Nat. Meth. 14: 587–589.

Krishnankutty, S. M. 2012. Systematics and biogeography of leafhoppers in Madagascar. PhD dissertation, University of Illinois, Urbana-Champaign.

Krishnankutty, S. M., C. H. Dietrich, W. Dai, and **M. Siddappaji. 2016**. Phylogeny and historical biogeography of leafhopper subfamily Iassinae (Hemiptera: Cicadellidae) with a revised tribal classification based on morphological and molecular data. Syst. Entomol. 41: 580–595.

Minh, B. Q., H. A. Schmidt, O. Chernomor, D. Schrempf, M. D. Woodhams, A. Von Haeseler, and **R. Lanfear. 2020**. IQ-TREE 2: new models and efficient methods for phylogenetic inference in the genomic era. Mol. Biol. Evol. 37: 533–534.

Nascimbene, P. and **H. Silverstein. 2000**. The preparation of fragile Cretaceous ambers for conservation and study of organismal inclusions, pp. 93–102. *In* D. A. Grimaldi (ed.), Studies on fossils in amber, with particular reference to the Cretaceous of New Jersey. Backhuys, Leiden.

Nguyen, L.-T., H. A. Schmidt, A. von Haeseler, and **B. Q. Minh. 2015**. IQ-TREE: a fast and effective stochastic algorithm for estimating maximum likelihood phylogenies. Mol. Biol. Evol. 32: 268–274.

Nixon, K. C. 2002. Winclada. Version 1.00.08. Published by the author. Ithaca, NY. http://www.cladistics.com/ [accessed on 10 August 2012].

Oman, P. W. 1937. Fossil Hemiptera from the Fox Hills sandstone (Cretaceous) of Colorado. J. Paleontol. 11: 38.

Oman, P. W., W. J. Knight, and **M. W. Nielson. 1990**. Leafhoppers (Cicadellidae): a bibliography, generic check-list, and index to the World Literature 1956–1985. C.A.B. International Institute of Entomology, Wallingford, U.K.

Peretti, A. 2021. An alternative perspective for acquisitions of amber from Myanmar including recommendations of the United Nations Human Rights Council. Int. J. Humanit. Action. 6: 12.

Poinar, G., Jr, and **A. Brown. 2020**. A new genus of leafhoppers (Hemiptera: Cicadellidae) in mid-Cretaceous Myanmar amber. Hist. Biol. 32: 160–163.

Rakitov, R. A. 1998. On differentiation of cicadellid leg chaetotaxy (Homoptera: Auchenorrhyncha: Membracoidea). Russian Entomol. J. 6: 7–27.

Ronquist, F., M. Teslenko, P. D. Mark, D. L. Ayres, A. Darling, S. Höhna, B. Larget, L. Liu, M. A. Suchard, and **J. P. Huelsenbeck. 2012**. MrBayes 3.2: efficient Bayesian phylogenetic inference and model choice across a large model space. Syst. Biol. 61: 539–542.

Ross, A. J. 2019. Burmese (Myanmar) amber checklist and bibliography 2018. Palaeoentomology. 2: 22–84.

Ross, A. J. 2020. Supplement to the Burmese (Myanmar) amber checklist and bibliography, 2019. Palaeoentomology. 3: 103–118.

Shcherbakov, D. E. 1986. Cicadina (= Auchenorrhyncha). 28: 47-50. *In* A.P. Rasnitsyn (ed.), Insects in the Early Cretaceous ecosystems of West Mongolia. Transactions of the Joint Soviet-Mongolian Palaeontological Expedition, Nauka, Moscow (in Russian).

Shcherbakov, D. E. 1992. The earliest leafhoppers (Hemiptera: Karajassidae n. fam.) from the Jurassic of Karatau. Neues. Jahrb. Geol. Palaontol. Abh. 1992: 39–51.

Shcherbakov, D. E. 2012. More on Mesozoic Membracoidea (Homoptera). Russ. Entomol. J. 21: 15–22.

Shi, G., D. A. Grimaldi, G. E. Harlow, J. Wang, J. Wang, M. Wang, W. Lei, Q. Li, and **X. Li. 2012**. Age constraint on Burmese amber based on UePb dating of zircons. Cretaceous Res. 37, 155–163.

Skidmore, R. E. 1999. Checklist of the Canadian amber inclusions in the Canadian National Collection of Insects, p. 244. Agriculture and Agri-Food Canada, Ottawa.

Skinner, R. K., C. H. Dietrich, K. K. O. Walden, E. Gordon, A. D. Sweet, L. Podsiadlowski, M. Petersen, C. Simon, D. M. Takiya, and **K. P. Johnson. 2019**. Phylogenomics of Auchenorrhyncha (Insecta: Hemiptera) using transcriptomes: examining controversial relationships via degeneracy coding and interrogation of gene conflict. Syst. Entomol. 45: 85–113.

Szwedo, J. 2005. *Jantarivacanthus kotejai* gen. et sp. n. from Eocene Baltic amber, with notes on the Bathysmatophorini and related taxa (Hemiptera: Cicadomorpha: Cicadellidae). Polish J. Entomol. 74: 251–276.

Szwedo, J., B. Wang, A. Soszyńska-Maj, D. Azar, A. J. Ross. 2020. International Palaeoentomological Society Statement. Palaeoentomol. 3: 221–222.

Takiya, D. M. and **C. H. Dietrich. 2017**. New species and new subfamily placement of the enigmatic Neotropical leafhopper tribe Neopsini (Hemiptera: Cicadellidae). Entomologica Americana 122(3): 435–450.

Wang, Y., C. H. Dietrich, and **Y. Zhang. 2017**. Phylogeny and historical biogeography of leafhopper subfamily Evacanthinae (Hemiptera: Cicadellidae) based on morphological and molecular data. Sci. Rep. 7: 45387.

Wang, X., C. H. Dietrich, and **Y. Zhang. 2019**. The first fossil Coelidiinae: a new genus and species from Myanmar amber (Hemiptera, Cicadellidae). Cretaceous Res. 95: 146–150.

Wei, C., Y. Zhang, and **C. H. Dietrich. 2010**. First record of the tribe Malmaemichungiini Kwon from China with description of a new species of the genus *Malmaemichungia* Kwon (Hemiptera: Cicadellidae). Zootaxa. 2689: 48–56.

Xue, Q., C. H. Dietrich and **Y. Zhang. 2020**. Phylogeny and classification of the leafhopper subfamily Eurymelinae (Hemiptera: Cicadellidae) inferred from molecules and morphology. Syst. Entomol. 45: 687–702.

Young, D. A. 1968. Taxonomic study of the Cicadellinae (Homoptera: Cicadellidae). Part 1. Proconiini. Bull. U. S. Nat. Mus. 261: 1–287.

Zahniser, J. N., and **C. H. Dietrich. 2010**. Phylogeny of the leafhopper subfamily Deltocephalinae (Hemiptera: Cicadellidae) based on molecular and morphological data with a revised family-group classification. Syst. Entomol. 35: 489–511.

Zahniser, J. N., and **C. H. Dietrich. 2013**. A review of the tribes of Deltocephalinae (Hemiptera: Auchenorrhyncha: Cicadellidae). European Journal of Taxonomy 45: 1–211.

Zhang, H. C. 1997. Early Cretaceous insects from the Dalazi Formation of the Zhixin basin, Jilin Province, China. Palaeoworld. 7: 75e103.